

## Research Paper

## Innovative design of a thermoelectric generator of extended legs with tapering and segmented pin configuration: Thermal performance analysis

Haider Ali <sup>a</sup>, Bekir Sami Yilbas <sup>a,b,\*</sup><sup>a</sup> Department of Mechanical Engineering, King Fahd University of Petroleum & Minerals, Dhahran 31261, Saudi Arabia<sup>b</sup> Center of Research Excellence in Renewable Energy, Research Institute, King Fahd University of Petroleum & Minerals, Dhahran 31261, Saudi Arabia

## HIGHLIGHTS

- Maximum efficiency depends on segmented and tapering configurations of pins.
- External load resistance and temperature ratios have effect on maximum device efficiency.
- Extended leg configuration enhances thermoelectric efficiency upto 8% increase.
- Output power is influenced by tapering, external load and temperature ratios.
- Output power corresponding to new innovative design remains higher than single material configurations.

## ARTICLE INFO

## Article history:

Received 3 November 2016

Revised 5 May 2017

Accepted 12 May 2017

Available online 17 May 2017

## Keywords:

Thermoelectric generator  
Pin tapering  
Segmented  
Extended leg  
Thermal analysis

## ABSTRACT

New design of a thermoelectric generator with extended pin configuration is introduced and its performance is assessed incorporating the pin tapering parameter and the operating conditions including external load and temperature ratios. The segmented configuration of device pins is also incorporated in the thermodynamic analysis. The device maximum efficiency and output power are formulated and analyzed for various values of the device design and operating parameters. It is found that the maximum efficiency of new innovative design of the thermoelectric generator remains higher than those previous designs incorporating single material pin configuration without tapering. Tapering of the pin geometry increases the maximum efficiency of the thermoelectric generator, particularly for low values of the external load parameter. The device output power of the extended leg thermoelectric generator with segmented configuration remains higher as compare to the thermoelectric generator with single pin material. A new innovative design of a pin configuration is presented in the study, which provides high performance of thermoelectric generator, this makes the thermoelectric generator one of the promising renewable energy devices for possible applications in future.

© 2017 Elsevier Ltd. All rights reserved.

## 1. Introduction

A large scale and effective utilization of renewable energy sources is essential to slow down the climate change and lower its adverse effect on the environment. Although several research studies have been carried out to develop efficient renewable energy devices, such as photovoltaic panels, volumetric receivers, wind turbines, thermoelectric generators, etc., the research studies on the development of high efficiency renewable energy devices

and multi-generation systems meeting the challenges of investment, cost-effective operation, and maintenance are still in progress. Improving the efficiency of renewable energy systems through enhancing waste heat recovery and utilization is also challenging in terms of the innovative design of high efficiency devices and minimization of operational cost at device level. Thermoelectric generators are the devices, which convert thermal energy directly into electrical energy without involving combustion and rotating parts. The innovative design of a thermoelectric generator becomes necessary because of its low thermal efficiency and narrow operational temperature ranges. The innovative design of a thermoelectric generator with the consideration of extended legs with pin tapering is promising for efficient operation of the device.

\* Corresponding author at: Department of Mechanical Engineering, King Fahd University of Petroleum &amp; Minerals, Dhahran 31261, Saudi Arabia.

E-mail address: [bsyilbas@kfupm.edu.sa](mailto:bsyilbas@kfupm.edu.sa) (B.S. Yilbas).

## Nomenclature

$A_0$	area of rectangular geometry of thermoelectric generator ( $\text{m}^2$ )	$T_{\text{int},n}$	temperature at the interface of two <i>n</i> -type materials (K)
$I$	electrical current (A)	$T_{\text{int},p}$	temperature at the interface of two <i>p</i> -type materials (K)
$k_{\text{eff},n}$	effective thermal conductivity of <i>n</i> -type semiconductor ( $\text{W}/\text{mK}$ )	$V$	voltage (V)
$k_{\text{eff},p}$	effective thermal conductivity of <i>p</i> -type semiconductor ( $\text{W}/\text{mK}$ )	$W$	power output of the thermoelectric generator (W)
$k_n$	thermal conductivity of <i>n</i> -type semiconductor ( $\text{W}/\text{mK}$ )	$ZT_{\text{avg}}$	dimensionless Figure of Merit (1/K)
$k_p$	thermal conductivity of <i>p</i> -type semiconductor ( $\text{W}/\text{mK}$ )	$\alpha_n$	Seebeck coefficient of <i>n</i> -type semiconductor (V/K)
$K_{\text{eff}}$	overall effective thermal conductance of thermoelectric generator (W/K)	$\alpha_{n,\text{eff.}}$	effective Seebeck coefficient of <i>n</i> -type leg of semiconductor (V/K)
$K_0$	reference thermal conductivity for thermoelectric generator (W/K)	$\alpha_p$	Seebeck coefficient of <i>p</i> -type semiconductor (V/K)
$L$	total length of the leg of thermoelectric generator (m)	$\alpha_{p,\text{eff.}}$	effective Seebeck coefficient of <i>p</i> -type leg of semiconductor (V/K)
$R_L$	external load resistance ( $\Omega$ )	$\bar{\alpha}_{\text{eff.}}$	overall effective Seebeck coefficient of the thermoelectric generator (V/K)
$R_n$	electrical resistance of <i>n</i> -type leg of semiconductor ( $\Omega$ )	$\mu_n$	(= $L_{n,1}/L$ ) dimensionless ratio of <i>n</i> -type material 1 to total length of thermoelectric generator
$R_p$	electrical resistance of <i>p</i> -type leg of semiconductor ( $\Omega$ )	$\mu_p$	(= $L_{p,1}/L$ ) Dimensionless ratio of <i>p</i> -type material 1 to total length of thermoelectric generator
$R_0$	reference electrical resistance ( $\Omega$ )	$\eta$	efficiency
$R_{\text{TEG}}$	overall electrical resistance in of the thermoelectric generator ( $\Omega$ )	$\xi$	dimensionless shape factor
$s$	shape factor of the thermoelectric leg (m)	$\sigma_p$	electrical conductivity of <i>p</i> -type semiconductor (S/m)
$T_1$	hot side temperature of the thermoelectric generator (K)	$\sigma_n$	electrical conductivity of <i>n</i> -type semiconductor (S/m)
$T_2$	cold side temperature of the thermoelectric generator (K)	$\theta$	(= $T_2/T_1$ ) dimensionless ratio of the low and high temperature of thermoelectric generator

This is because of the fact that extended pins can operate independently at two low temperature sinks. This arrangement can improve the thermal efficiency of the system while tapering of the segmented pin configuration further contributes to the device efficiency enhancement. Consequently, it becomes necessary to perform the thermal analysis of a thermoelectric generator having extended legs with segmented and tapered pin configuration.

Considerable research was performed to study the thermoelectric generator performance under the different operating conditions. Thermoelectric power generator with segmented leg configuration was studied by Li et al. [1]. They showed that the electrical resistance of the segmented legs was dramatically increased in comparison with that of the bulk materials, which was due to the large interfacial resistance between different segments in the thermoelectric generator legs; therefore, the interfacial resistance was one of the key factors limiting the output power of the segmented thermoelectric generator. Segmented thermoelectric generator with tapered pin configuration was studied by Ali et al. [2]. They observed that segmentation of thermoelectric generator enhances the thermal performance of thermoelectric generator as compared with the non-segmented thermoelectric generator. In addition, they introduced the shaped factor related to the tapering of the pin of the thermoelectric generator. Their study revealed that increasing the tapering of pin thermoelectric result in the enhancement of the efficiency of the thermoelectric generator. However, at the same time, the device output power adversely effected by an increment in the shape factor. The design configuration of a thermoelectric generator incorporating the length ratio of segmented pins was performed by Zhang et al. [3]. Their finding reveals that for specific operating condition and configuration there exist a segmentation ratio which can provide the maximum thermal efficiency of thermoelectric generator. The comparative study for the performance assessment of the segmented and the traditional thermoelectric generators was carried out by Tian et al. [4]. Their results indicated that the increment in the pin length effect adversely on the device thermal

efficiency and output power. The maximum output power varied linearly with the pin cross-sectional area. For the waste heat recovery application, the segmented thermoelectric generator is more effective as compared to the traditional thermoelectric generator. Tian et al. [5] introduced the thermal analysis of a segmented thermoelectric generator, which designed for the heat recovery from diesel engine exhaust. They simulated the effect of operating temperatures, geometric configuration, and segmentation ratio on the device efficiency and power output. Their finding reveals that for high temperature heat source the thermoelectric generator with segmentation performed better as compared with to the traditional thermoelectric generator. Ming et al. [6] carried out the study to assess the thermal performance of the segmented thermoelectric generator. The findings from the thermal analysis reveal that their thermoelectric design provides the steady voltage, and maximum thermal efficiency is around 11.2%. The thermoelectric generators with segmentation were examined for their mechanical performances by Jia and Gao [7]. Their finding reveals that for given operating temperature of the segmented thermoelectric generator the requirements of mechanical strength is not satisfied. In addition, the segmented thermoelectric generator could not attain the design value of thermal efficiency. The design analysis of a thermoelectric generator with segmented was introduced by Kim et al. [8]. They assembled two-pair segmented  $\pi$ -shaped thermoelectric generator, contact resistance across the interface is low. The reported the peak specific power density as 42.9 W/kg for the temperature of 498 °C, their measurements and predicted analytical prediction are in good agreement. Hadjistassou et al. [9] presented the design configuration for high efficiency thermoelectric generators with segmentation. In the case of segmented  $\text{Bi}_2\text{Te}_3$ -PbTe the Seebeck coefficient is higher as compare to traditional thermoelectric generators made of  $\text{Bi}_2\text{Te}_3$  and PbTe. El-Genk et al. [10] studied the segmented thermoelectric generators for space power applications. Their study reveals that thermoelectric generator with segmentation can attain the 14.7% thermal efficiency for the cold side temperature of 300 K. The performance of a flat-plate

solar thermoelectric generator for space applications was studied by Liu et al. [11]. They demonstrated that adjusting the geometry of thermoelectric can provide the stable output, for high intensity radiation, as compared to the photovoltaic devices. A review study has been carried out by Orr et al. [12] for the application of thermoelectric generator with heat pipes in relation to the waste heat recovery systems of the car. They indicated that the use of heat pipes could potentially reduce the thermal resistance and pressure losses in the system as well as temperature regulation of the thermoelectric generators and increased design flexibility. In addition, thermoelectric generators had limitations such as low temperature limits and relatively low efficiencies. On the other hand, heat pipes had also limitations such as maximum rates of heat transfer and temperature limits.

Thermoelectric generators have low efficiencies because of limitations of material conversion factor such as Figure of Merit. This is mainly because of the poor electrical conductivity to thermal conductivity ratio of thermoelectric materials. Research into thermoelectric material development is still progressing to meet with requirements of high Figure of Merit towards achieving high thermoelectric device efficiency. The thermoelectric device efficiency and output power can be improved via innovative design of the device geometric configurations, such as pin tapering, and segmented pin arrangements [13,14]. However, the new design incorporating the extended pin configuration allows the device to operate between two different cold junction temperatures. The new consideration of extended pins of the thermoelectric generator initiates the innovative design of the device while allowing two cold junction temperatures in operation. Although device performance characteristics were investigated for pin tapering [13] and pin segmentation [14], the performance analysis of extended pin configuration having tapered geometric and segmented arrangements was left for future. Therefore, in the present study, a new design configuration of thermoelectric pins is incorporated to account for improving device efficiency and output power. Consequently, extended leg and segmented tapered pin configuration of the thermoelectric generator pins are introduced and thermal analysis of a new pins configuration is carried out. The new design of the leg extension is allowed to operate the device at two different low temperature junctions. The thermal performance of thermoelectric generator is formulated and simulated for various operating parameters including the external load parameter, temperature ratio, and pin taper angle.

## 2. Thermal analysis

In thermal analysis, the extended leg thermoelectric generator with tapered and segmented pin configuration is considered. Fig. 1 shows the schematic view of the segmented thermoelectric

generator. The thermal efficiency for the segmented configuration of the thermoelectric generator can be represented as [15]:

$$\eta = \frac{I^2 R_L}{\alpha_{eff.,1} T_{high} I + (\Delta T_{n,1} K_{n,1} + \Delta T_{p,1} K_{p,1}) - \frac{1}{2} I^2 (R_{n,1} + R_{p,1})} \quad (1)$$

where  $I$  represents the current,  $R_L$  represents the external electrical resistance,  $\alpha_{eff.,1} = \alpha_{p,1} - \alpha_{n,1}$ ,  $\alpha_{p,1}$  represents the Seebeck Coefficient for  $p$  type material 1,  $\alpha_{n,1}$  represents the Seebeck Coefficient for  $n$  type material 1,  $T_{high}$  is the temperature of high junction,  $K_{n,1}$  represents the thermal conductance of  $n$ -type material 1 and  $K_{p,1}$  represents the thermal conductance of  $n$ -type material 2.  $\Delta T_{n,1} = T_{high} - T_{int,n}$  where  $T_{int,n}$  is the temperature at the interface of two  $n$  type materials and  $\Delta T_{p,1} = T_{high} - T_{int,p}$ , where  $T_{int,p}$  is the temperature at the interface of two  $p$  type materials.  $R_{n,1}$  and  $R_{p,1}$  represent the electrical resistance of  $n$  type material 1 and  $p$  type material 1, respectively.

The current  $I$  can be given as:

$$I = \frac{V}{R_{TEG} + R_L} \quad (2)$$

where  $R_{TEG}$  is the electrical resistance in thermoelectric generator and  $V$  is the voltage across the thermoelectric power generator, which can be represented as:

$$V = (\alpha_{p,1} \Delta T_{p,1} + \alpha_{p,2} \Delta T_{p,2}) - (\alpha_{n,1} \Delta T_{n,1} + \alpha_{n,2} \Delta T_{n,2}) \quad (3)$$

where  $\Delta T_{n,1} = T_{high} - T_{int,n}$ ,  $\Delta T_{n,2} = T_{int,n} - T_{low,n}$  in which  $T_{int,n}$  is the  $n$ -interface temperature and  $\Delta T_{p,1} = T_{high} - T_{int,p}$ ,  $\Delta T_{p,2} = T_{int,p} - T_{low,p}$  in which  $T_{int,p}$  is the  $p$ -interface temperature.

In the thermoelectric generator, the tapered leg is considered as shown in Fig. 1. The variation in the cross-sectional area can be given as:

$$A(x) = A_0 + \left( x - \frac{L}{2} \right) s \quad (4)$$

where  $A_0$  represent the area in the case of a rectangular cross section of the leg,  $L$  represents total leg length, and  $s$  represents the shape factor which is given as:

$$s = \frac{dA}{dx} \quad (5)$$

Using the Fourier Law and incorporating the steady-state heat flow for the  $n$ -type leg.

$$Q = -k_{n,1} A \frac{dT}{dx} \quad \text{or} \quad Q \int_0^{L_{n,1}} \frac{dx}{A(x)} = -k_{n,1} \int_{T_{high}}^{T_{int,n}} dT \quad (6)$$

The above equation becomes:

$$Q \frac{L}{A_0 \xi} \ln \left( \frac{1 + \xi \mu_n - \xi/2}{1 - \xi/2} \right) = k_{n,1} (T_{high} - T_{int,n}) \quad (7)$$

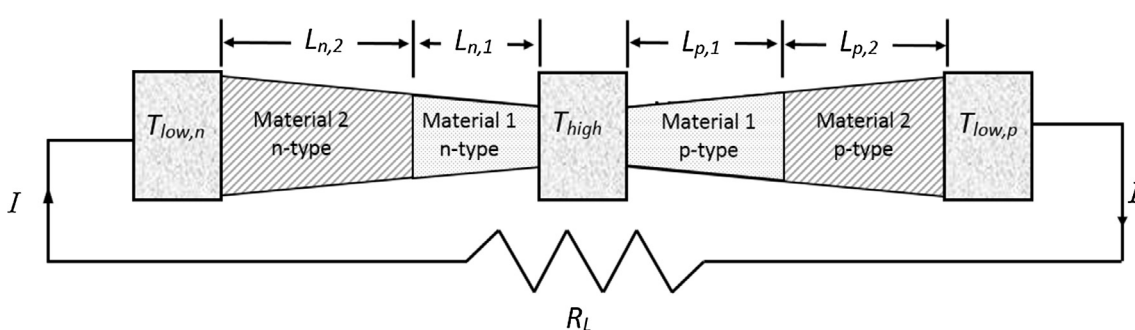


**Fig. 1.** A schematic view of the extended length thermoelectric generator with segmented and tapered pin configuration. Material 1 is modified lead telluride and material 2 is modified bismuth telluride.

where  $\mu_n (= L_{n,1}/L)$  represents the dimensionless length of  $n$ -type material 1, and  $\xi$  represent the dimensionless shape factor, which can be given as:

$$\xi = \frac{L_s}{A_0} \quad (8)$$

For the complete pin leg, the Fourier Law can be given by:

$$Q = k_{n,eff} A_0 \frac{(T_{high} - T_{low,n})}{L} \quad (9)$$

Now comparing Eqs. (9) and (7) results into the following:

$$\Delta T_{n,1} = \frac{k_{n,eff} (T_{high} - T_{low,n})}{k_{n,1} \xi} \ln \left( \frac{1 + \xi \mu_n - \xi/2}{1 - \xi/2} \right) \quad (10)$$

where  $k_{n,eff}$  is the effective thermal conductivity of  $n$ -type leg,  $k_{n,1}$  is the thermal conductivity of  $n$ -type material 1.

Similarly,

$$\Delta T_{n,2} = \frac{k_{n,eff} (T_{high} - T_{low,n})}{k_{n,2} \xi} \ln \left( \frac{1 + \xi/2}{1 + \xi \mu_n - \xi/2} \right) \quad (11)$$

where  $k_{n,2}$  is the thermal conductivity of  $n$ -type material 2.

Similarly,

$$\Delta T_{p,1} = \frac{k_{p,eff} (T_{high} - T_{low,p})}{k_{p,1} \xi} \ln \left( \frac{1 + \xi \mu_p - \xi/2}{1 - \xi/2} \right) \quad (12)$$

and,

$$\Delta T_{p,2} = \frac{k_{p,eff} (T_{high} - T_{low,p})}{k_{p,2} \xi} \ln \left( \frac{1 + \xi/2}{1 + \xi \mu_p - \xi/2} \right) \quad (13)$$

where  $\mu_p (= L_{p,1}/L)$  represents the dimensionless length in the case of  $p$ -type material 1,  $k_{p,eff}$ . represents the effective thermal conductivity of  $p$ -type leg,  $k_{p,1}$  is the thermal conductivity of  $p$ -type material 1 and  $k_{p,2}$  is the thermal conductivity of  $p$ -type material 2.

Eq. (3) can be given as:

$$V = \left( \alpha_{p,1} \frac{k_{p,eff}}{k_{p,1} \xi} \ln \left( \frac{1 + \xi \mu_p - \xi/2}{1 - \xi/2} \right) + \alpha_{p,2} \frac{k_{p,eff}}{k_{p,2} \xi} \ln \left( \frac{1 + \xi/2}{1 + \xi \mu_p - \xi/2} \right) (T_{high} - T_{low,p}) \right. \\ \left. - \left( \alpha_{n,1} \frac{k_{n,eff}}{k_{n,1} \xi} \ln \left( \frac{1 + \xi \mu_n - \xi/2}{1 - \xi/2} \right) + \alpha_{n,2} \frac{k_{n,eff}}{k_{n,2} \xi} \ln \left( \frac{1 + \xi/2}{1 + \xi \mu_n - \xi/2} \right) (T_{high} - T_{low,n}) \right) \right) \quad (14)$$

The effective Seebeck Coefficient for  $p$  and  $n$  type materials are defined as:

$$\alpha_{p,eff} = \left( \alpha_{p,1} \frac{k_{p,eff}}{k_{p,1} \xi} \ln \left( \frac{1 + \xi \mu_p - \xi/2}{1 - \xi/2} \right) + \alpha_{p,2} \frac{k_{p,eff}}{k_{p,2} \xi} \ln \left( \frac{1 + \xi/2}{1 + \xi \mu_p - \xi/2} \right) \right) \quad (15)$$

and

$$\alpha_{n,eff} = \left( \alpha_{n,1} \frac{k_{n,eff}}{k_{n,1} \xi} \ln \left( \frac{1 + \xi \mu_n - \xi/2}{1 - \xi/2} \right) + \alpha_{n,2} \frac{k_{n,eff}}{k_{n,2} \xi} \ln \left( \frac{1 + \xi/2}{1 + \xi \mu_n - \xi/2} \right) \right) \quad (16)$$

The overall effective Seebeck Coefficient can be given as:

$$\bar{\alpha}_{eff} = \alpha_{p,eff} - \alpha_{n,eff} \quad (17)$$

Eq. (14) becomes:

$$V = \alpha_{p,eff} (T_{high} - T_{low,p}) - \alpha_{n,eff} (T_{high} - T_{low,n}) \quad (18)$$

Now, using Eq. (18) into Eq. (2) results into the following:

$$I = \frac{\alpha_{p,eff} (T_{high} - T_{low,p}) - \alpha_{n,eff} (T_{high} - T_{low,n})}{R_{TEG} + R_L} \quad (19)$$

Now considering  $T_{low,p} = T_{low}$  and  $T_{low,n} = T_{low,p} - \Delta T_{low,p-n} = T_{low} - \Delta T_{low,p-n}$ , Eq. (19) can be re-written as:

$$I = \lambda \frac{\bar{\alpha}_{eff} (T_{high} - T_{low})}{R_{TEG} + R_L} \quad (20)$$

where

$$\lambda = 1 - \frac{\alpha_{n,eff} \Delta T_{low,p-n}}{\bar{\alpha}_{eff} (T_{high} - T_{low})} \quad (21)$$

The total electrical resistance, is the summation of  $n$  and  $p$  type leg resistance, which can be given as:

$$R_{TEG} = R_n + R_p \quad (22)$$

where  $R_n$  represents the electric resistance  $n$  type leg of thermoelectric generator and  $R_p$  represents the electric resistance  $p$  type leg of thermoelectric generator.

$$R_n = \int_0^{L_{n,1}} \frac{dx}{\sigma_{n,1} A(x)} + \int_{L_{n,1}}^L \frac{dx}{\sigma_{n,2} A(x)} \quad (23)$$

Integration of Eq. (23), results into following:

$$R_n = \frac{L}{\xi A_0 \sigma_{n,1}} \ln \left( \frac{1 + \xi \mu_n - \xi/2}{1 - \xi/2} \right) + \frac{L}{\xi A_0 \sigma_{n,2}} \times \ln \left( \frac{1 + \xi/2}{1 + \xi \mu_n - \xi/2} \right) \quad (24)$$

Similarly,

$$R_p = \frac{L}{\xi A_0 \sigma_{p,1}} \ln \left( \frac{1 + \xi \mu_p - \xi/2}{1 - \xi/2} \right) + \frac{L}{\xi A_0 \sigma_{p,2}} \times \ln \left( \frac{1 + \xi/2}{1 + \xi \mu_p - \xi/2} \right) \quad (25)$$

Now, Eq. (22) becomes:

$$R_{TEG} = \left( \frac{L}{\xi A_0 \sigma_{n,1}} \ln \left( \frac{1 + \xi \mu_n - \xi/2}{1 - \xi/2} \right) + \frac{L}{\xi A_0 \sigma_{n,2}} \ln \left( \frac{1 + \xi/2}{1 + \xi \mu_n - \xi/2} \right) + \frac{L}{\xi A_0 \sigma_{p,1}} \ln \left( \frac{1 + \xi \mu_p - \xi/2}{1 - \xi/2} \right) + \frac{L}{\xi A_0 \sigma_{p,2}} \ln \left( \frac{1 + \xi/2}{1 + \xi \mu_p - \xi/2} \right) \right) \quad (26)$$

Now, introducing the following parameters:

Reference thermal conductance:

$$K_0 = \frac{k_{n,1@300K} A_0}{L} \quad (27)$$

Reference electrical resistance:

$$R_0 = \frac{L}{\sigma_{n,1@300K} A_0} \quad (28)$$

Temperature ratio:

$$\theta = \frac{T_{low}}{T_{high}} \quad (29)$$

Overall effective thermal conductance:

$$\bar{K}_{eff} = k_{n,eff} \left( \frac{A_n}{L_n} \right) + k_{p,eff} \left( \frac{A_p}{L_p} \right) \quad (30)$$

Dimensionless Figure of Merit:

$$ZT_{avg} = \frac{(\bar{\alpha}_{eff})^2 T_{high}}{R_{TEG} \bar{K}_{eff}} \left( \frac{1 + \theta}{2} \right) \quad (31)$$

When incorporating parameters which are mentioned above into Eq. (1), results into the following:

$$\eta = \frac{2 ZT_{avg} (1 - \theta) \left( \frac{R_L}{R_0} \right)}{2 \left( \frac{1}{\lambda} \right) \left( \frac{Z_{eff,1}}{\bar{\alpha}_{eff}} \right) \left( \frac{R_{TEG}}{R_0} + \frac{R_L}{R_0} \right) ZT_{avg} + (1 + \theta) \left( \frac{1}{R_{TEG}/R_0} \right) \left( \frac{\gamma}{\lambda^2} \right) \left( \frac{R_{TEG}}{R_0} + \frac{R_L}{R_0} \right)^2 - 2 ZT_{avg} (1 - \theta) \left( \frac{R_{n,1} + R_{p,1}}{R_0} \right)} \quad (32)$$

where

$$\gamma = 1 + \frac{k_{n,\text{eff}} \cdot A_n}{K_{\text{eff}} \cdot L_n} \frac{\Delta T_{\text{low},p-n}}{(T_{\text{high}} - T_{\text{low}})} \quad (33)$$

The power output of the thermoelectric power generator is given as:

$$W = I^2 R_L \quad (34)$$

Introducing the  $I$  from Eqs. (20) and (27) to (30) one can get the following.

$$\frac{W}{K_0 T_{\text{low}}} = \frac{2 Z T_{\text{avg}} \lambda^2 \theta (1 - \theta)^2 \frac{\bar{K}_{\text{eff}}}{K_0} \frac{R_{\text{TEG}}}{R_0} \frac{R_L}{R_0}}{(1 + \theta) \left( \frac{R_{\text{TEG}}}{R_0} + \frac{R_L}{R_0} \right)^2} \quad (35)$$

For material 1, the temperature dependent properties of modified lead telluride (n-type -  $\text{Ag}_{0.8}\text{Pb}_{19+x}\text{SbTe}_{20}$ : p-type -  $\text{Ag}_{0.9}\text{Pb}_9\text{Sn}_9\text{Sb}_{0.6}\text{Te}_{20}$ ) are incorporated. Whereas, the temperature dependent properties of modified bismuth telluride (n-type -  $\text{Bi}_2\text{Te}_{3-x}\text{Se}_x$  : p-type -  $\text{Bi}_x\text{Sb}_{2-x}\text{Te}_3$ ) are introduced as material 2. Table 1 represents the temperature dependent properties of modified lead and bismuth telluride [16].

For the comparison of the thermal performance of the suggested tapered segmented and extended thermoelectric power generator with the non-segmented thermoelectric generators, some dimensionless ratios are introduced, which are given below.

Efficiency Ratio:

$$\zeta_{\eta,1} = \frac{\eta_1}{\eta_{\max}} \quad (36)$$

and

$$\zeta_{\eta,2} = \frac{\eta_2}{\eta_{\max}} \quad (37)$$

Output Power Ratio:

$$\zeta_{W,1} = \frac{W_1}{W_{\max}} \quad (38)$$

and

$$\zeta_{W,2} = \frac{W_2}{W_{\max}} \quad (39)$$

where  $\eta_{\max}$  is the maximum efficiency which can achieved in the case of segmented and extended thermoelectric power generator,  $\eta_1$  and  $\eta_2$  represent the efficiency of the thermoelectric when material 1 and 2 are analyzed without segmentation respectively,  $W_{\max}$

is the maximum device output power which one can obtain in the case of segmented and extended thermoelectric generator,  $W_1$  and  $W_2$  represent the device output power when only material 1 and 2 are analyzed without segmentation respectively. MATLAB is developed to solve the derived equation. Fig. 2 represents the flow chart for the thermal analysis of thermoelectric generator. The simulation matrix is provided into Table 2.

### 3. Validation and comparison with classical pin design

In order to perform the validation study for the computer code developed for the thermal performance, the available experimental data in the open literature is considered [8]. The simulation is performed according to the operating conditions reported in the experimental study [8]. The segmented thermoelectric generator thermal efficiency is simulated and the findings are compared to those presented in the previous study [8]. Fig. 3 shows the predicted and experimental efficiencies [8]. It can be seen that simulation and experimental results are matching well with some small discrepancies. The difference between predictions of efficiency and the experimental data is in the order of 8%. In this case, the present simulations predict higher values of efficiency than the experimental data [8]. This may be attributed to one or all of the followings: (i) experimental error, which is in the order of 6%, and (ii) the interfacial resistance between the pins and source plates, which is incorporated in the analysis as the estimated value rather than the exact value. Nevertheless, the discrepancy between the predictions and experimental data is small and the increasing trend of both efficiencies is almost identical.

The comparison of thermal efficiencies of the conventional design of a thermoelectric generator (paralleled pins configuration with single pin material) and a new design configuration is shown in Fig. 4. It should be noted that the new design incorporates both modified bismuth telluride and modified lead telluride materials in the device pins and these materials are incorporated individual in the analysis of the conventional design and corresponding efficiencies are provided in the figure. Thermal efficiency of the conventional design, incorporating the individual pin material, remains less than thermal efficiency of the new design for all values of the external load parameter ( $R_L/R_0$ ) and both temperature ratios ( $\theta$ ). Although efficiency improvement is within 1–1.5%, the overall percentage (efficiency improved over the device efficiency) is more than 10%.

**Table 1**

Properties of Modified Lead and Bismuth Telluride [16] used in simulations ( $T$  is the temperature in K).

**Material: n-type Modified Lead Telluride  $\text{Ag}_{0.8}\text{Pb}_{19+x}\text{SbTe}_{20}$**

Electrical conductivity (S/cm)

Seebeck coefficient ( $\mu\text{V/K}$ )

Thermal conductivity (W/m/K)

**Material: p-type Modified Lead Telluride  $\text{Ag}_{0.9}\text{Pb}_9\text{Sn}_9\text{Sb}_{0.6}\text{Te}_{20}$**

Electrical conductivity (S/cm)

Seebeck coefficient ( $\mu\text{V/K}$ )

Thermal conductivity (W/m/K)

**Material: n-type Modified Bismuth telluride  $\text{Bi}_2\text{Te}_{3-x}\text{Se}_x$**

Electrical conductivity (S/cm)

Seebeck coefficient ( $\mu\text{V/K}$ )

Thermal conductivity (W/m/K)

**Material: p-type Modified Bismuth telluride  $\text{Bi}_x\text{Sb}_{2-x}\text{Te}_3$**

Electrical conductivity (S/cm)

Seebeck coefficient ( $\mu\text{V/K}$ )

Thermal conductivity (W/m/K)

$$\begin{aligned} \sigma &= 1462 - 10.419T + 0.031315T^2 - 4.0429 \times 10^{-5}T^3 + 1.9034 \times 10^{-8}T^4 \\ \alpha &= 173.26 - 3.8229T + 0.011679T^2 - 1.5584 \times 10^{-5}T^3 + 7.6695 \times 10^{-9}T^4 \\ k &= 0.6586 + \frac{329.63}{T} + \frac{22145}{T^2} \end{aligned}$$

$$\begin{aligned} \sigma &= 179.02 + 12.336T - 0.042167T^2 + 5.129 \times 10^{-5}T^3 - 2.1435 \times 10^{-8}T^4 \\ \alpha &= 1450 - 10.36T + 0.03123T^2 - 4.038 \times 10^{-5}T^3 + 1.903 \times 10^{-8}T^4 \\ k &= 0.56959 + \frac{550.66}{T} - \frac{47483}{T^2} \end{aligned}$$

$$\begin{aligned} \sigma &= -2139.4 + 2.5778T + e^{12.795 - 0.89098 \ln(T)} \\ \alpha &= 443.49 - 4.5121T + 9.4424 \times 10^{-3}T^2 - 5.8362 \times 10^{-6}T^3 \\ k &= -4.6205 + 9.9277 \times 10^{-3}T + \frac{833.7}{T} + \frac{23536}{T^2} \end{aligned}$$

$$\begin{aligned} \sigma &= -473.1 + 0.86507T + e^{16.637 - 1.6942 \ln(T)} \\ \alpha &= -188.2 + 2.2411T - 3.0075 \times 10^{-3}T^2 + 2.4914 \times 10^{-7}T^3 \\ k &= -1.8067 + 2.7529 \times 10^{-3}T - \frac{64.639}{T} + \frac{1.3395 \times 10^5}{T^2} \end{aligned}$$

#### 4. Results and discussion

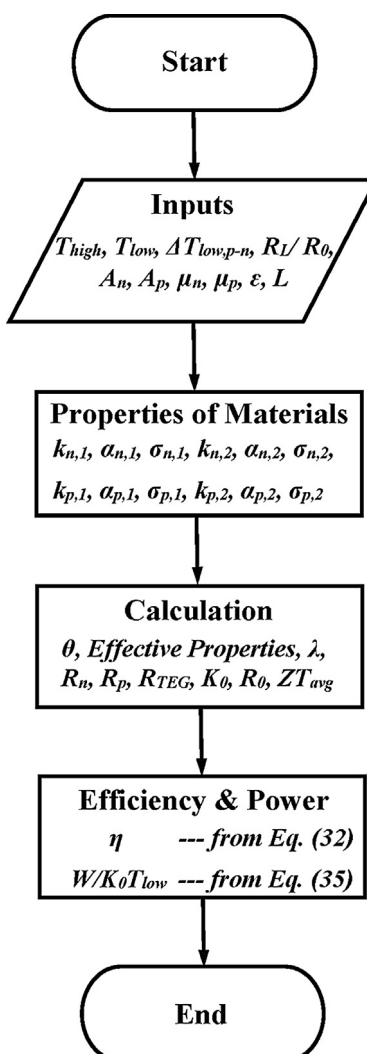
The innovative design of tapered thermoelectric generator with extended and segmentation is considered. The thermal efficiency of the thermoelectric generator and output power are examined incorporating the various values of the operational parameters such as external load parameter and temperature ratio.

The variation of leg length ratio for n-type ( $\mu_n = L_{n,1}/L$ , where  $L_{n,1}$  represents the length of the n-type of pin of the first material - n-type -  $Ag_{0.8}Pb_{19+x}SbTe_{20}$ : p-type -  $Ag_{0.9}Pb_9Sn_9Sb_{0.6}Te_{20}$  - and  $L$  is the total pin length (Fig. 1) and p-type ( $\mu_p = L_{p,1}/L$ , where  $L_{p,1}$  represents the length of the p-type of pin of the first material - n-type -  $Bi_2Te_{3-x}Se_x$ : p-type -  $Bi_xSb_{2-x}Te_3$  - and  $L$  is the total pin length (Fig. 1)) pins with pin tapering parameter maximizing the device efficiency is predicted. The findings are shown in Figs. 5a and 5b and for two values of the cold junction temperature ( $\Delta T_{low,p-n} = T_{low,p} - T_{low,n}$ , where  $T_{low}$  represents the cold junction temperature and indices 1 and 2 correspond to the first and second pin, respectively) and various external load parameter ( $R_L/R_0$ , where  $R_L$  is the external load resistance and  $R_0$  is the reference load resistance of the thermoelectric generator, and  $\sigma_{n,1@300K}$  electrical conductivity of n-type pin material of the first kind at reference

temperature, 300 K). Due to the segmentation in the legs of thermoelectric generators, two materials are present (Fig. 1). The first and second materials are the modified lead telluride (n-type -  $Ag_{0.8}Pb_{19+x}SbTe_{20}$ : p-type -  $Ag_{0.9}Pb_9Sn_9Sb_{0.6}Te_{20}$ ) and the modified bismuth telluride (n-type -  $Bi_2Te_{3-x}Se_x$ : p-type -  $Bi_xSb_{2-x}Te_3$ ), respectively. In general, the length ratio maximizing the device efficiency reduces with increasing tapering of the segmented pin configuration. This situation alters with the external load ratio. The external load ratio depends on the resistance of the external devices, which are connected to the thermoelectric generator. Therefore, depending on the operational conditions, the device maximum efficiency varies. Consequently, the thermoelectric generator design should be based on the spectrum of well-defined operational conditions rather than random considerations of the range of the operational parameters. However, the decrease of pin length ratio with the tapering parameter indicates that the pin tapering is a critical geometric parameter to improve the device efficiency. In this case, increasing pin tapering alters the length ratio of the pins while influencing the maximum efficiency.

Figs. 6a and 6b show the pin length ratio as similar to those in Figs. 5a and 5b while maximizing the device work output. The trend of variation of the pin length ratio with the tapering parameter is similar to those shown in Figs. 5a and 5b, provided the slope of decay of the length ratio with the tapering parameter is not same as those shown in Figs. 5a and 5b. Hence, the pin configuration maximizing the device efficiency does not maximize the device output power. Consequently, when designing the thermoelectric power generator with extended legs of tapering and segmented pin configuration, one need to decide either the maximum device efficiency or the device output power that matters for the practical applications, i.e., the pin length ratio changes according to the requirements of the maximum device efficiency or the maximum device output power. The surface plot of the efficiency and output power with the pin length ratio are shown in Figs. 7a and 7b for various values of the tapering parameter. The pin length ratio maximizing the device output power does not maximize the device efficiency for same operational conditions in terms of external load ratio and temperature parameter ( $\theta = T_2/T_1$ , where  $T_2$  is the cold junction temperature and  $T_1$  is the hot junction temperature).

Figs. 8a and 8b show the device maximum efficiency with a tapering parameter of the pin for different cold junction temperature difference, various values of the external load ratio, and two temperature ratios, respectively. Figs. 9a and 9b show the surface plot of the maximum efficiency with the tapering parameter and cold junction temperature differences for several values of the external load ratio and two temperature differences, respectively. The maximum efficiency attains relatively higher values when the tapering parameter differs from zero. The zero tapering parameter corresponds to the parallel pin configurations of the thermoelectric generator. Therefore, tapering of the pins improves the maximum efficiency of the device. However, in the case of low temperature ratio ( $\theta = T_2/T_1$ , where  $T_2$  and  $T_1$  are low and high junction temperatures of the thermoelectric generator) results in a small improvement in the maximum efficiency with tapering for the low external load ratio ( $R_L/R_0$ ). Reducing the external load ratio gives rise to high values of the device maximum efficiency in line with Eq. (32); in which case, the efficiency is proportional to the first power of the external load ratio, but inversely proportional to the square of the external load ratio. Since the thermoelectric power generation is proportional to the external load ( $I^2 R_L$ ), the lowering external load reduces the output power. This, in turn, improves the device efficiency for low values of the external load or external load ratio ( $R_L/R_0$ , where  $R_0$  remains constant for specific design consideration). The innovative design of the

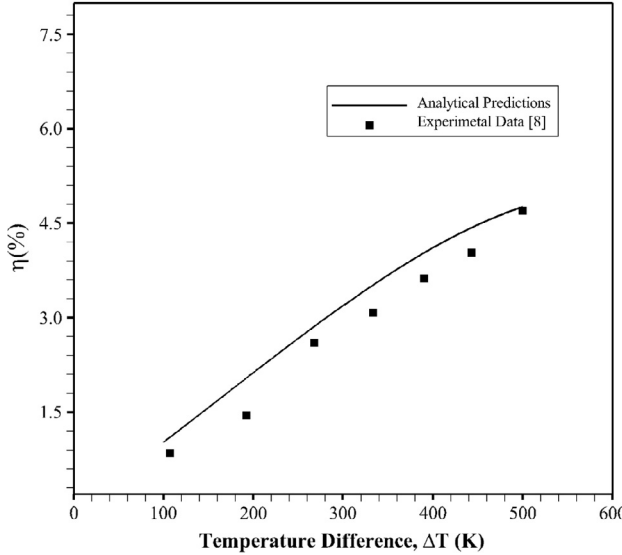


**Fig. 2.** The flow chart representing the thermal analysis of the thermoelectric generator.

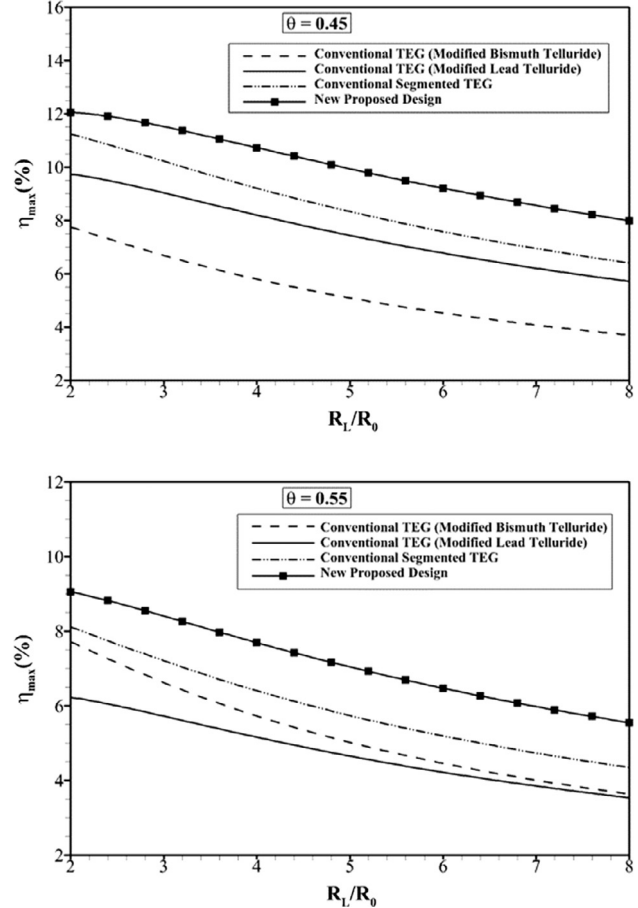
**Table 2**

Parameters used in the simulation.

$L$	$A^a$	$T_{low}$	$\theta$	$R_L/R_0$	$\mu_n, \mu_p$	$\xi$	$\Delta T_{low,p-n}$
4 mm	16 mm <sup>2</sup>	300 K	0.45–0.55	2–8	0–1	–1.5 to 1.5	0–20

<sup>a</sup> For conventional TEGs.**Fig. 3.** The comparison of efficiency of thermoelectric generator from the present study and previous experimental study [8].

external leg configuration operating at two different cold junction temperatures significantly improves the device maximum efficiency. In this case, increasing temperature difference at the cold junction ends of the device pins increases the maximum efficiency. This is true for a whole range of temperature and external load ratios used in the simulations. On the other hand, in order to assess the improvement of the device efficiency when extended and segmented fin configurations used, the ratio of the efficiency of the device due to simple pin configuration to the maximum efficiency of the current pin configuration ( $\zeta_{\eta,1} = \frac{\eta_1}{\eta_{max}}$  and  $\zeta_{\eta,2} = \frac{\eta_2}{\eta_{max}}$ , where  $\eta_1$  and  $\eta_2$  are the efficiency corresponding to the simple pin configuration with no segmentation when material type one - modified lead telluride (n-type -  $Ag_{0.8}Pb_{19+x}SbTe_{20}$ : p-type -  $Ag_{0.9}Pb_9Sn_9Sb_{0.6}Te_{20}$ ) - is used and when material type 2 - modified bismuth telluride (n-type -  $Bi_2Te_{3-x}Se_x$  : p-type -  $Bi_xSb_{2-x}Te_3$ ) - is used, respectively and  $\eta_{max}$  is the maximum efficiency due to current pin configuration) is computed for various operating conditions. The findings are shown in Figs. 10a and 10b for various operating conditions. It should be noted that since two different thermoelectric materials are used in the segmented pin configuration, the simulation for the efficiency of the simple fin configuration is repeated for two materials and the efficiencies are identified as  $\eta_1$  and  $\eta_2$ . The efficiency ratios due to both materials remain less than unity, it is more noticeable for tapered pin configuration. This is true for the efficiency ratio corresponding to the first material (modified lead telluride (n-type -  $Ag_{0.8}Pb_{19+x}SbTe_{20}$ : p-type -  $Ag_{0.9}Pb_9Sn_9Sb_{0.6}Te_{20}$ )). This indicates that the new design of tapering of segmented thermoelectric generator enhanced the thermal efficiency of the device, particularly for the large external load ratio ( $R_L/R_0 > 2$ ) and low temperature ratio ( $\theta = 0.45$ ). However, in the case of the second material (modified bismuth telluride (n-type -  $Bi_2Te_{3-x}Se_x$  : p-type -  $Bi_xSb_{2-x}Te_3$ )), tapering slightly increases the efficiency ratio. Therefore, the tapered configuration

**Fig. 4.** Thermal efficiency of thermoelectric generators with external load parameter ( $R_L/R_0$ ) for two temperature ratios ( $\theta$ ). The conventional design incorporates paralleled pins and single pin material.

has an opposing effect on the efficiency improvement. Nevertheless, the efficiency ratio remains less than unity while indicating that the new innovative design results in higher efficiency than the classical design with a single thermoelectric generator. The increase of temperature difference at the cold junction due to extended pin configuration further lowers the efficiency ratio. Consequently, the new innovative design of the thermoelectric generator provides the enhanced thermal efficiency of the device almost for all the operating conditions considered.

Figs. 11a and 11b show the dimensional device output power with the tapering parameter (shape factor,  $\xi = Ls/A_0$ ) for various operating conditions including external load ( $R_L/R_0$ ) and temperature ( $\theta = T_2/T_1$ ) ratios while Figs. 12a and 12b show the surface plots of the dimensionless device output power with the temperature difference between the cold junctions of the extended pins and the tapering parameter. The device output power reduces with tapering of the pin configuration unlike the device efficiency (Figs. 8a and 8b). However, the reduction in the device output power is not considerably high for tapering, which is in the order of 8%. This reduction further reduces with increasing external load

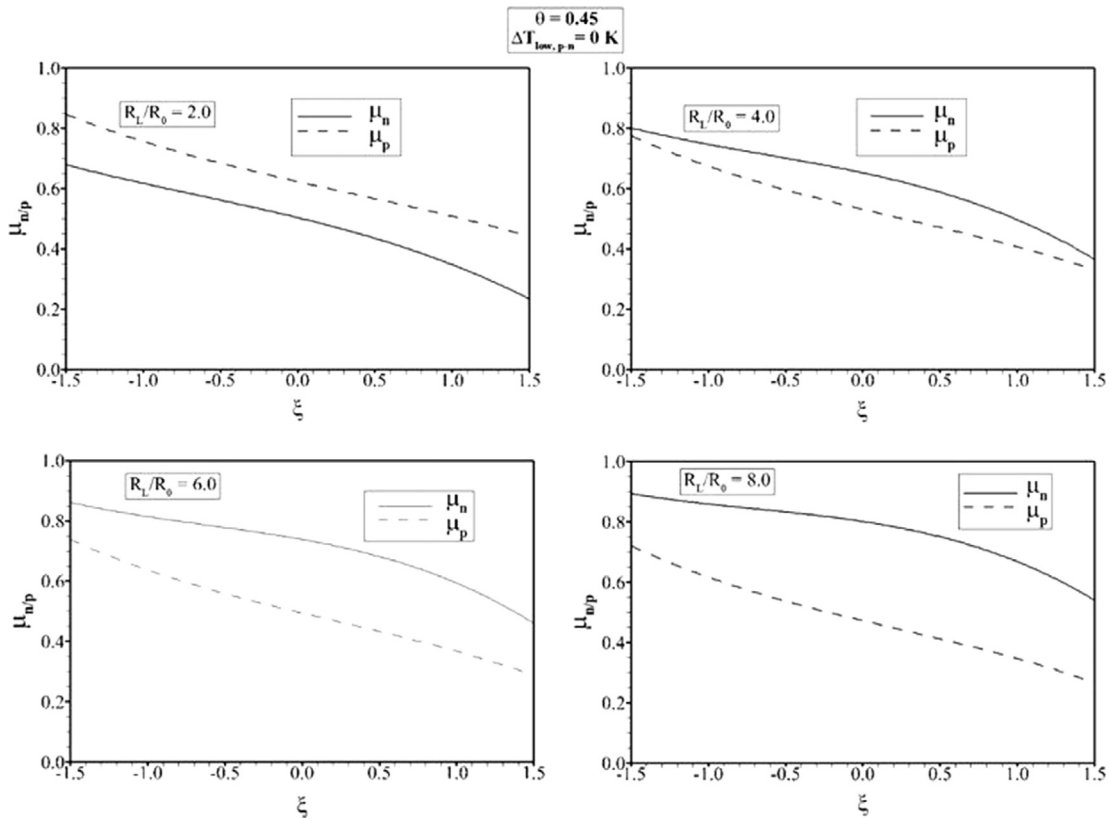


**Fig. 5a.** Variation of leg length ratio for n and p-types ( $\mu_{n/p} = L_{n/p,1}/L$ ) of pin with pin tapering for various values of the external load ratio ( $R_L/R_0$ ) and two cold junction temperature difference ( $\Delta T_{cold}$ ) of zero. The length ratio maximizes the device efficiency.

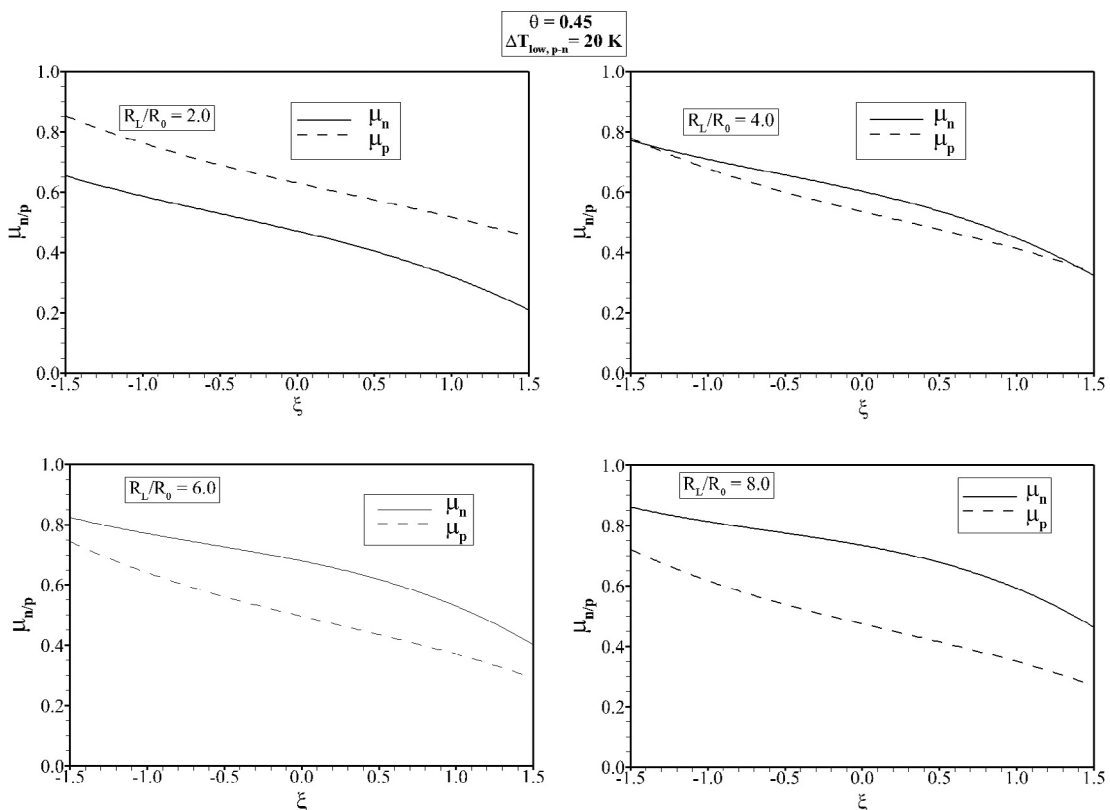


**Fig. 5b.** Variation of leg length ratio for n and p-types ( $\mu_{n/p} = L_{n/p,1}/L$ ) of pin with pin tapering for various values of the external load ratio ( $R_L/R_0$ ) and two cold junction temperature difference ( $\Delta T_{cold}$ ) of 20 K. The length ratio maximizes the device efficiency.

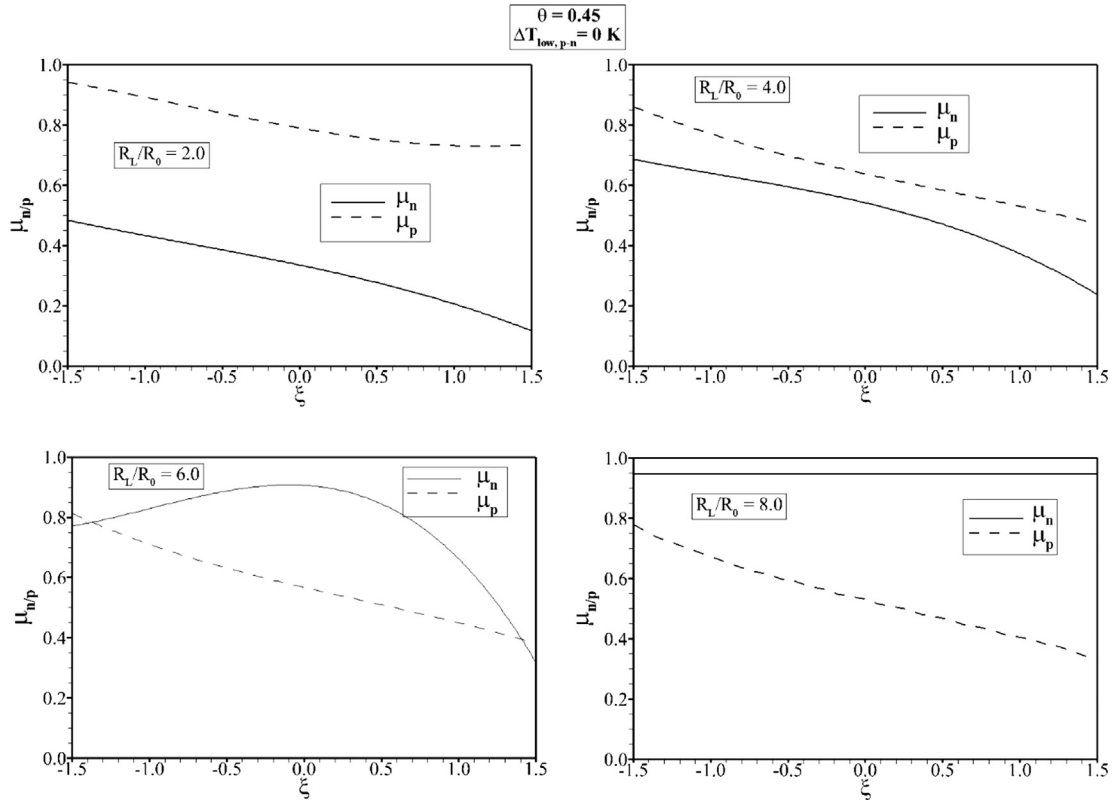


**Fig. 6a.** Variation of leg length ratio for n and p-types ( $\mu_{n/p} = L_{n/p,1}/L$ ) of pin with pin tapering for various values of the external load ratio ( $R_L/R_0$ ) and two cold junction temperature difference ( $\Delta T_{cold}$ ) of zero. The length ratio maximizes the device output work.

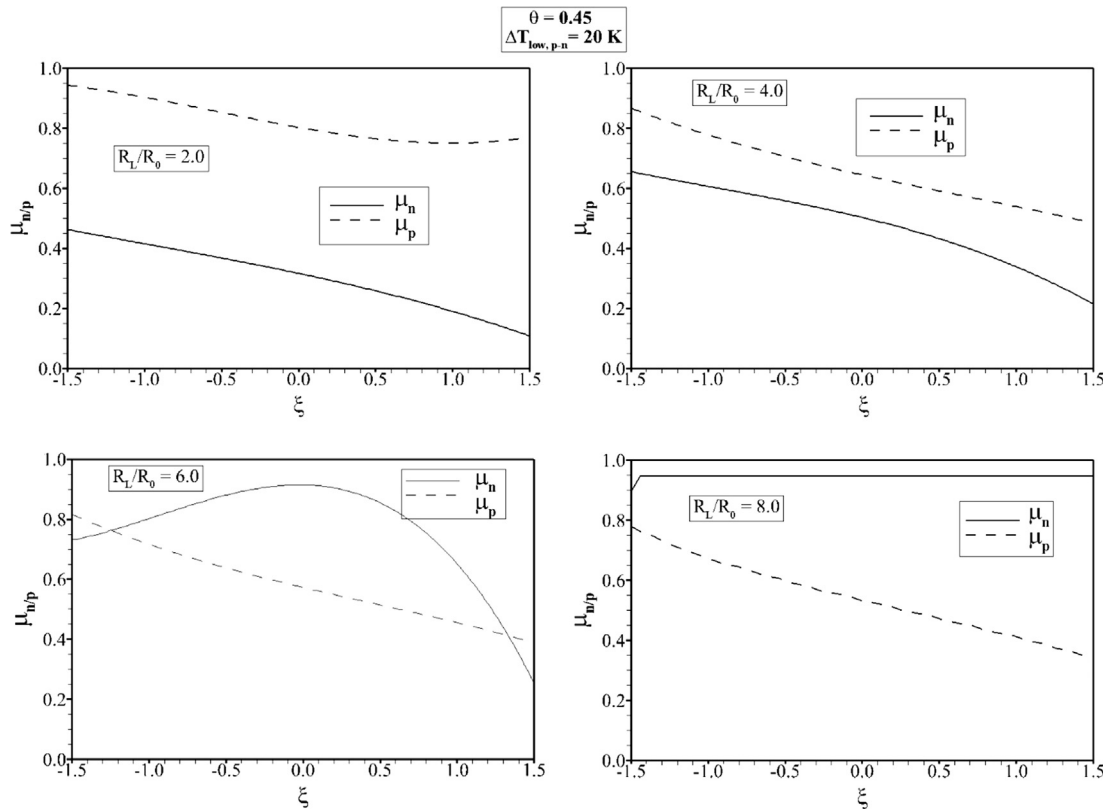


**Fig. 6b.** Variation of leg length ratio for n and p-types ( $\mu_{n/p} = L_{n/p,1}/L$ ) of pin with pin tapering for various values of the external load ratio ( $R_L/R_0$ ) and two cold junction temperature difference ( $\Delta T_{cold}$ ) of 20 K. The length ratio maximizes the device output work.

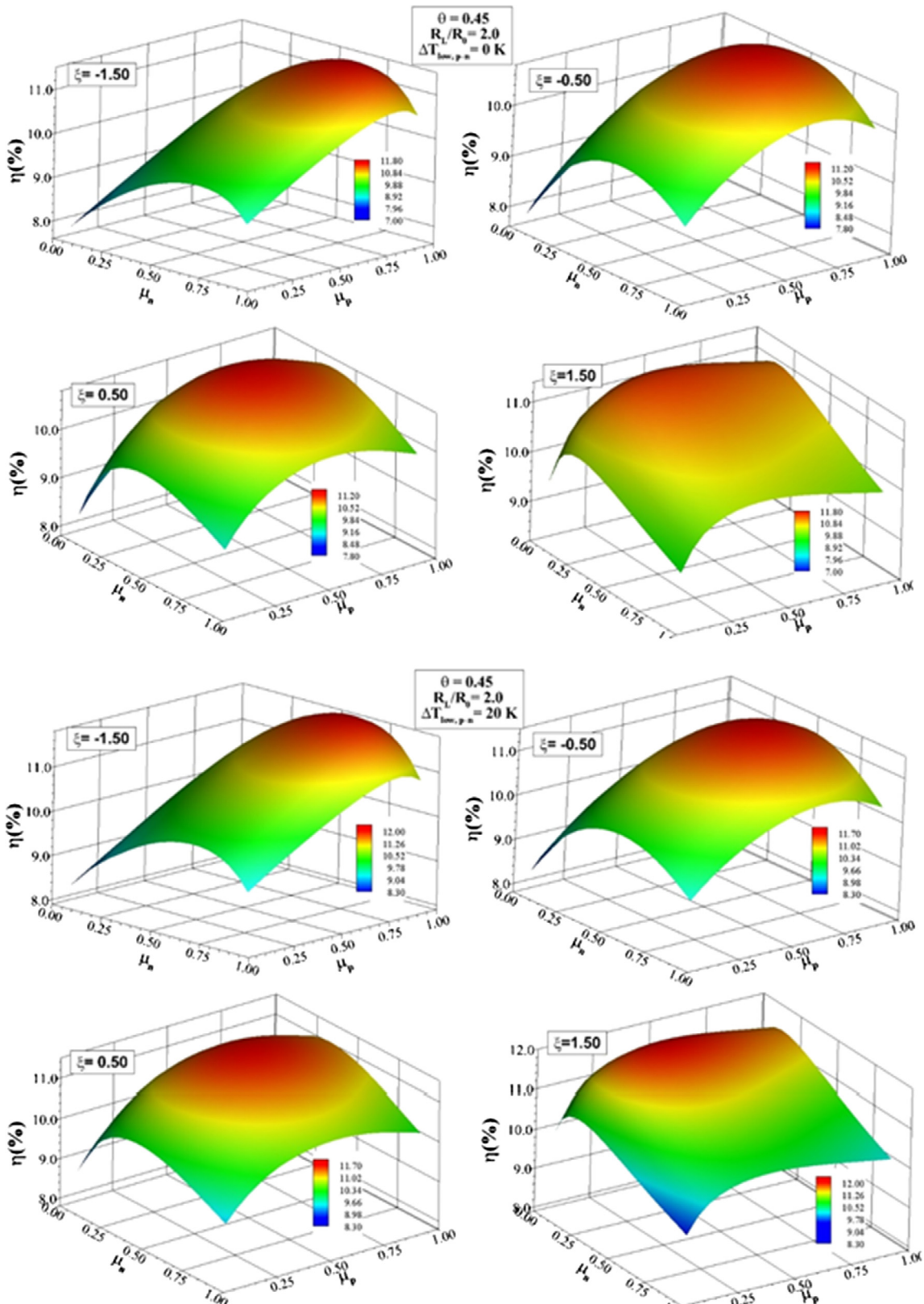


**Fig. 7a.** Surface plot of device efficiency for various values of tapering parameters.

ratio and increasing temperature ratio. This behavior is attributed to the useful work ( $I^2 R_L$ ), which increases with the external load resistance. On the other hand, increasing temperature difference between the cold junctions of the extended pins also lowers the

device output power. This reduction is small, which is in the order of 4%. In order to assess the device output power due to the new innovative design of the pin configuration with those corresponding to the classical design incorporating a single material pin

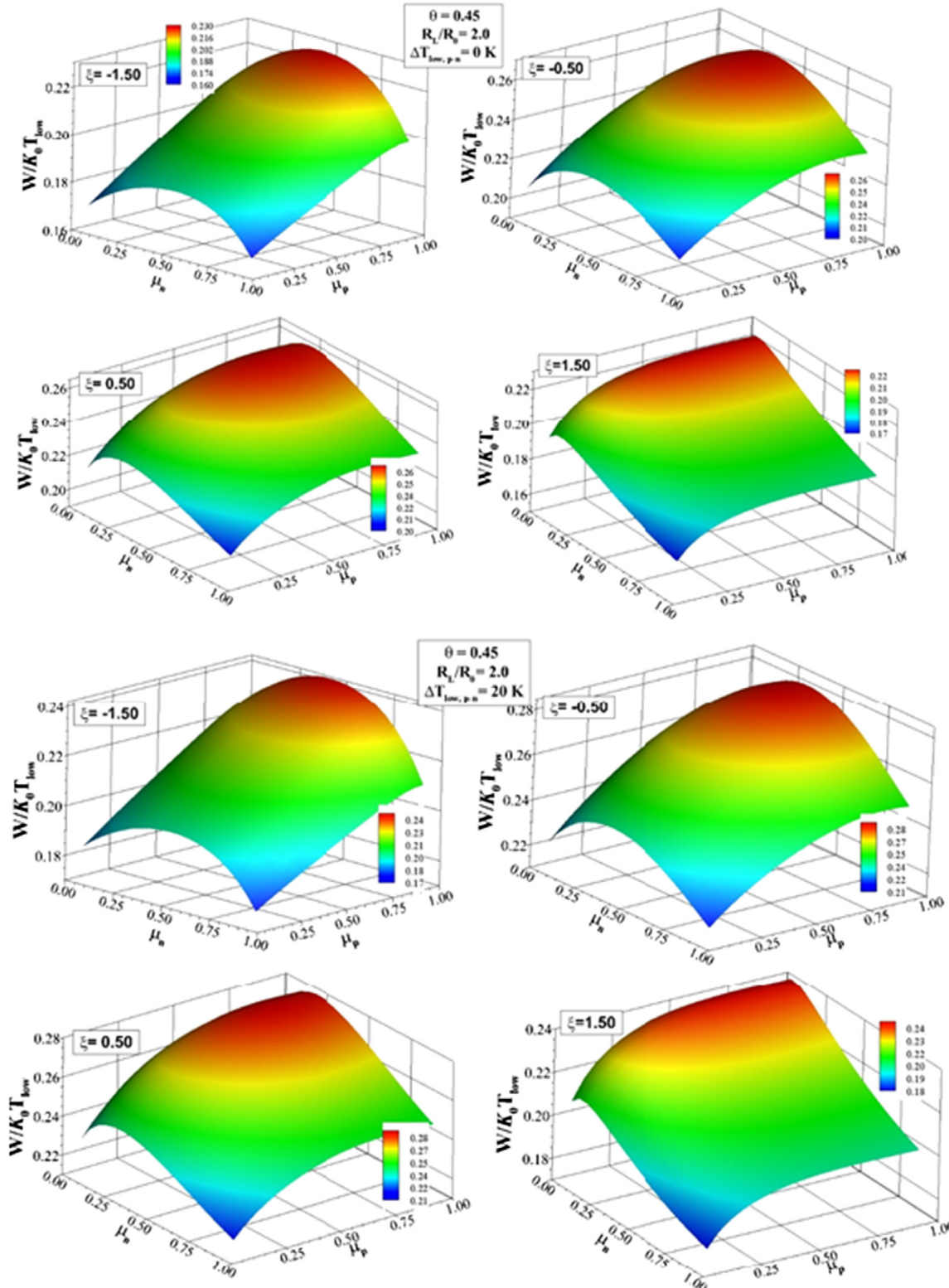


**Fig. 7b.** Surface plot of device output work for various values of tapering parameters.

configuration, the output power ratios are introduced. In this case, the power output ratio of  $\zeta_{W,1} = \frac{W_1}{W_{max}}$  corresponds to the ratio of the power output when thermoelectric generator has a single pin material of the first type to the power output when new design configuration is introduced. Similarly, the power output ratio of  $\zeta_{W,2} = \frac{W_2}{W_{max}}$  power output when thermoelectric generator has a sin-

gle pin material of the second type material to the power output when current design configuration is introduced.

Figs. 13a and 13b show the output power ratios with taper parameter for various external load and temperature ratios. The power output ratio remains less than unity for both materials considered. This indicates that the new innovative design of the ther-

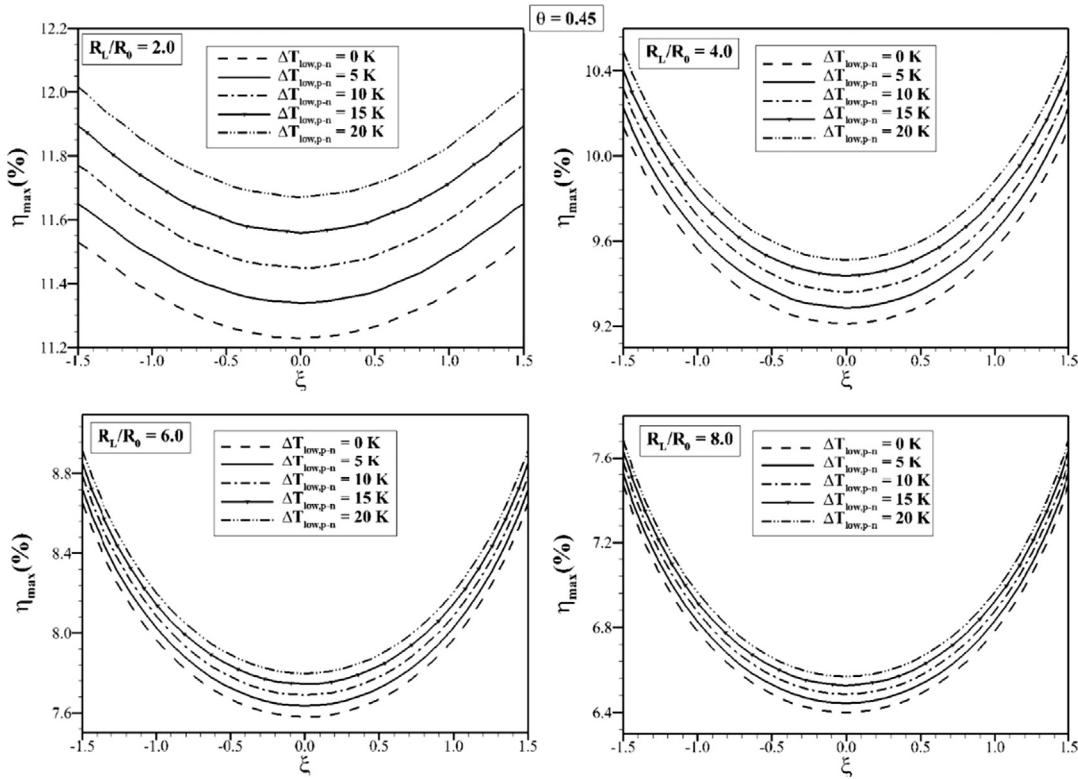


**Fig. 8a.** Variation of the maximum device efficiency with tapering parameter for values of various external load ratio and cold junction temperature differences for temperature ratio  $\theta = 0.45$ .

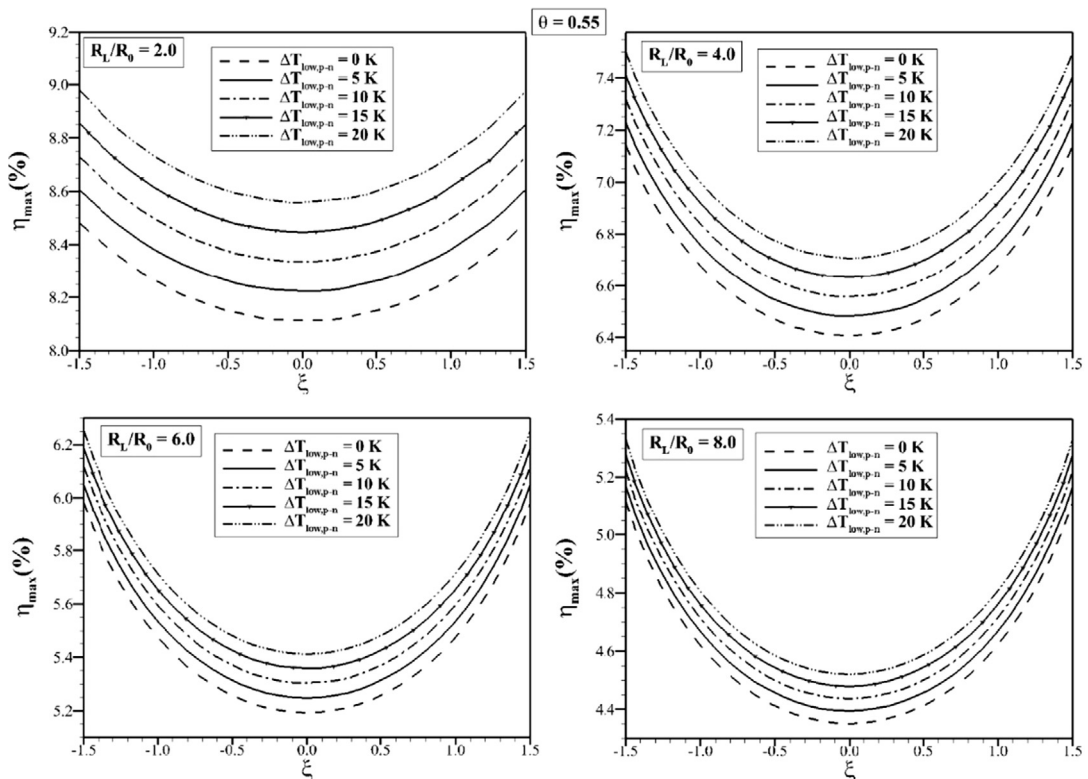


**Fig. 8b.** Variation of the maximum device efficiency with tapering parameter for values of various external load ratio and cold junction temperature differences for temperature ratio  $\theta = 0.55$ .

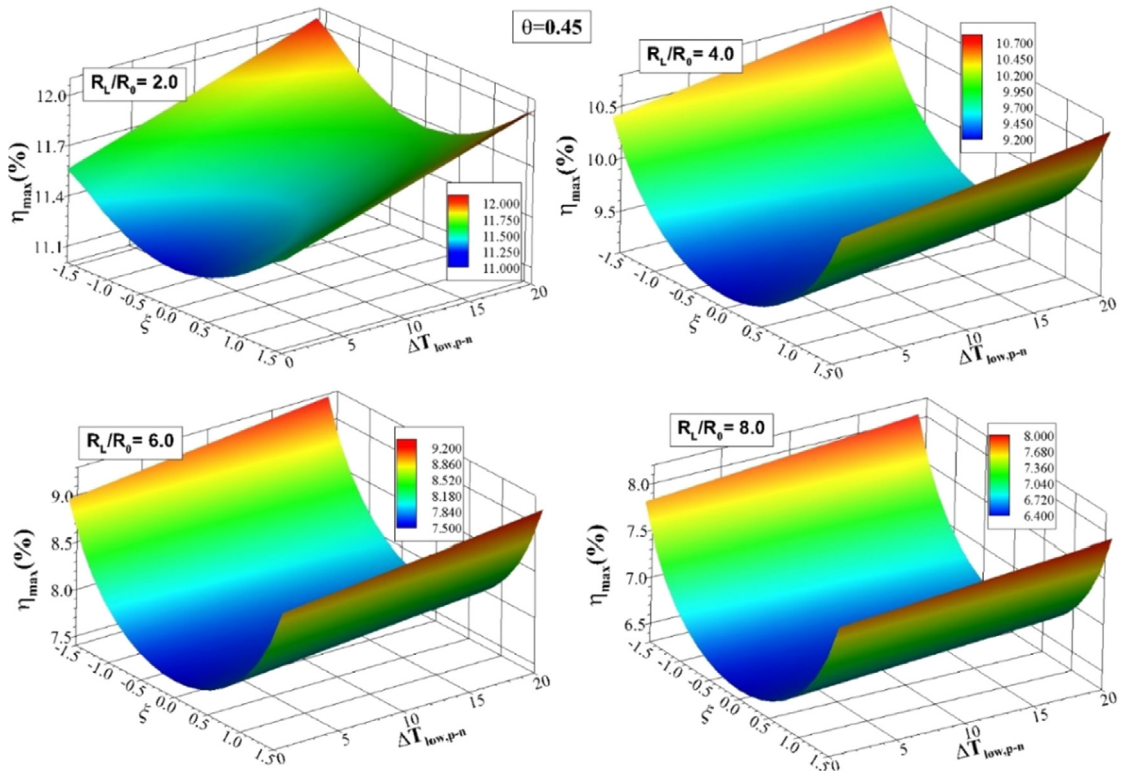


**Fig. 9a.** Surface plot of the maximum device maximum efficiency with tapering parameter ((shape factor,  $\xi = Ls/A_0$ ) and cold junction temperature differences for values of various external load ratio for temperature ratio  $\theta = 0.45$ .

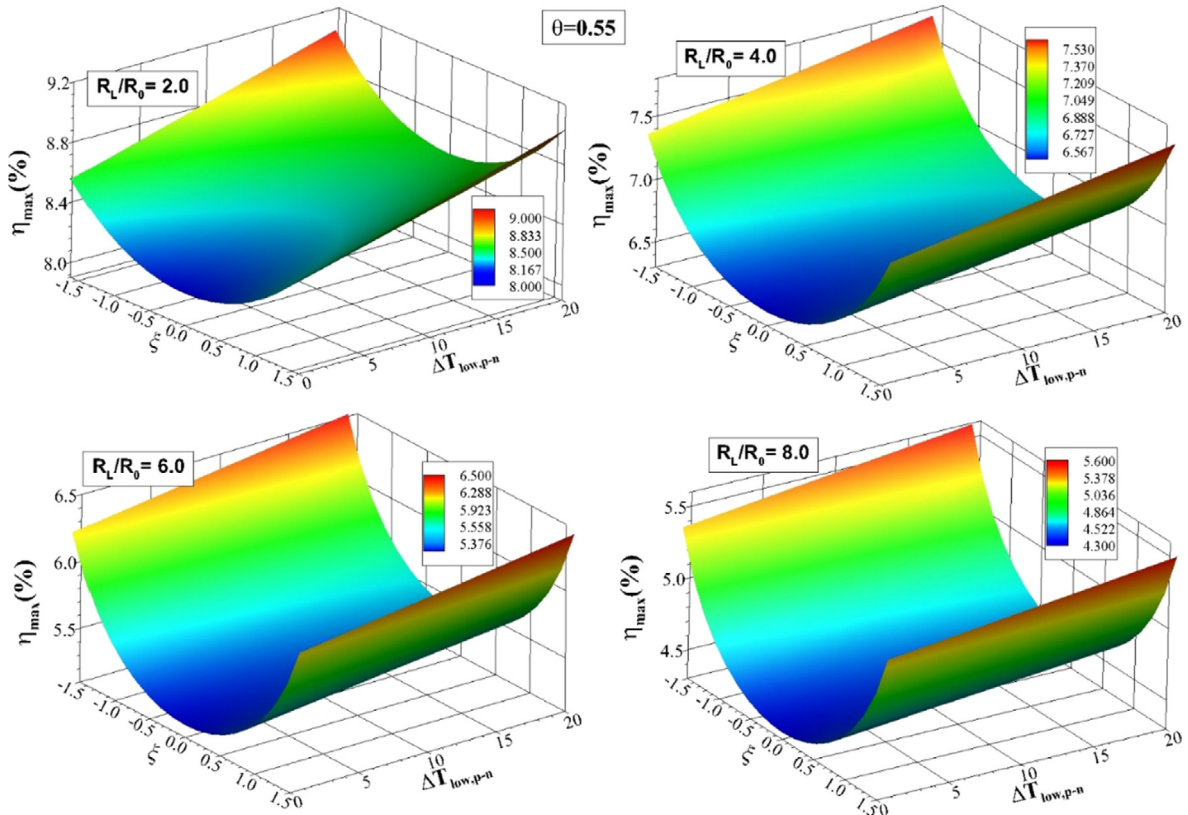


**Fig. 9b.** Surface plot of the maximum device maximum efficiency with tapering parameter (shape factor,  $\xi = Ls/A_0$ ) and cold junction temperature differences for values of various external load ratio for temperature ratio  $\theta = 0.55$ .

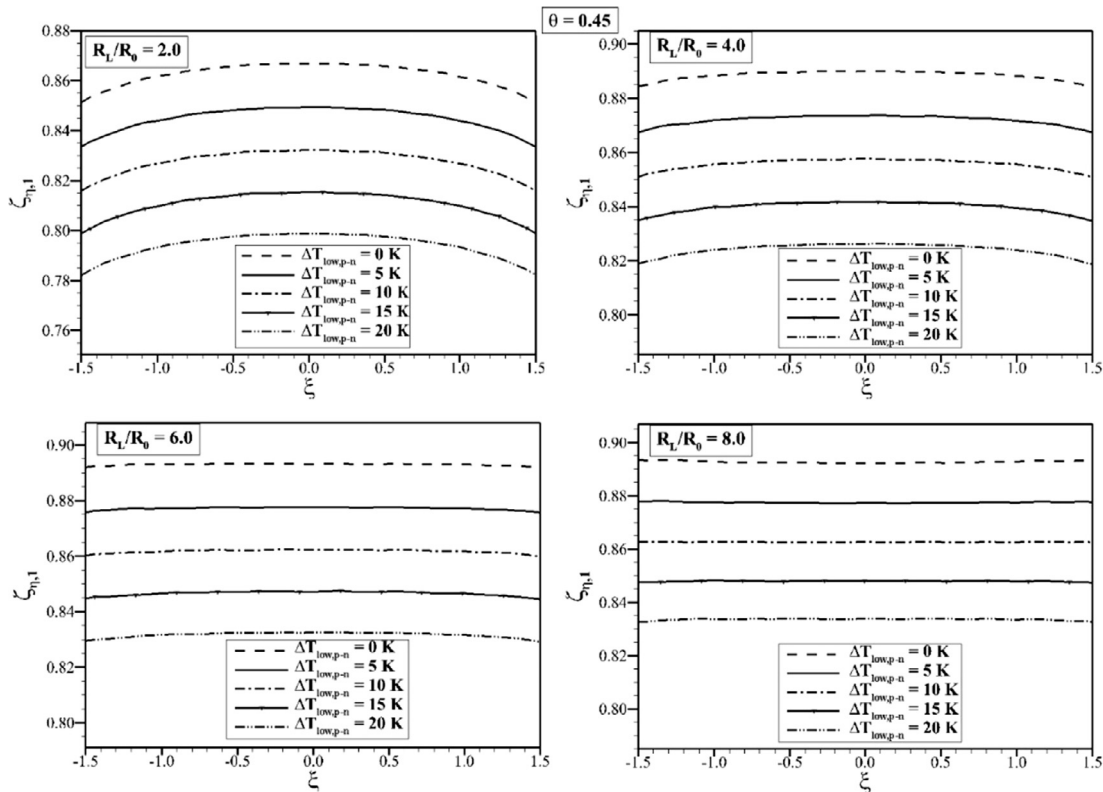


**Fig. 10a.** Variation of the efficiency ratio ( $\zeta_{\eta_1} = \eta_1/\eta_{\max}$ , where  $\eta_1$  efficiency corresponding to the simple pin configuration - modified lead telluride) with tapering parameter for values of various external load ratio and cold junction temperature differences for temperature ratio  $\theta = 0.45$ .

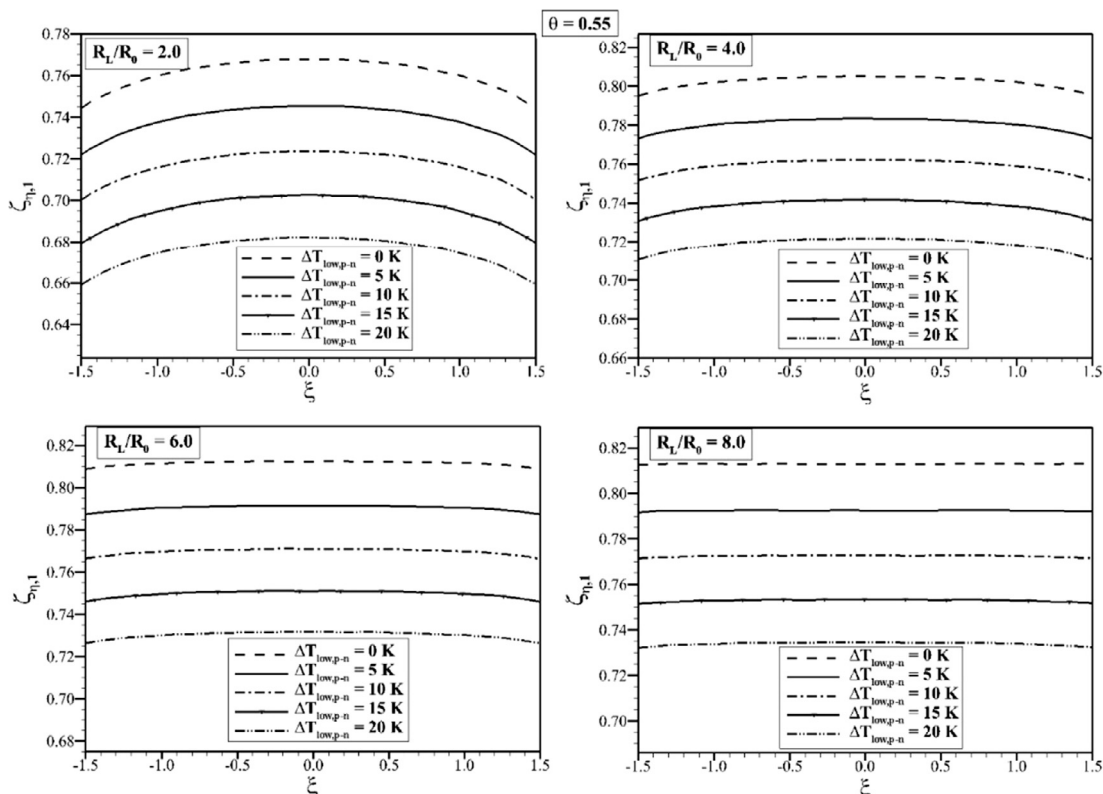


**Fig. 10b.** Variation of the efficiency ratio ( $\zeta_{\eta_1} = \eta_1/\eta_{\max}$ , where  $\eta_1$  efficiency corresponding to the simple pin configuration - modified lead telluride) with a tapering parameter for values of various external load ratio and cold junction temperature differences for temperature ratio  $\theta = 0.55$ .

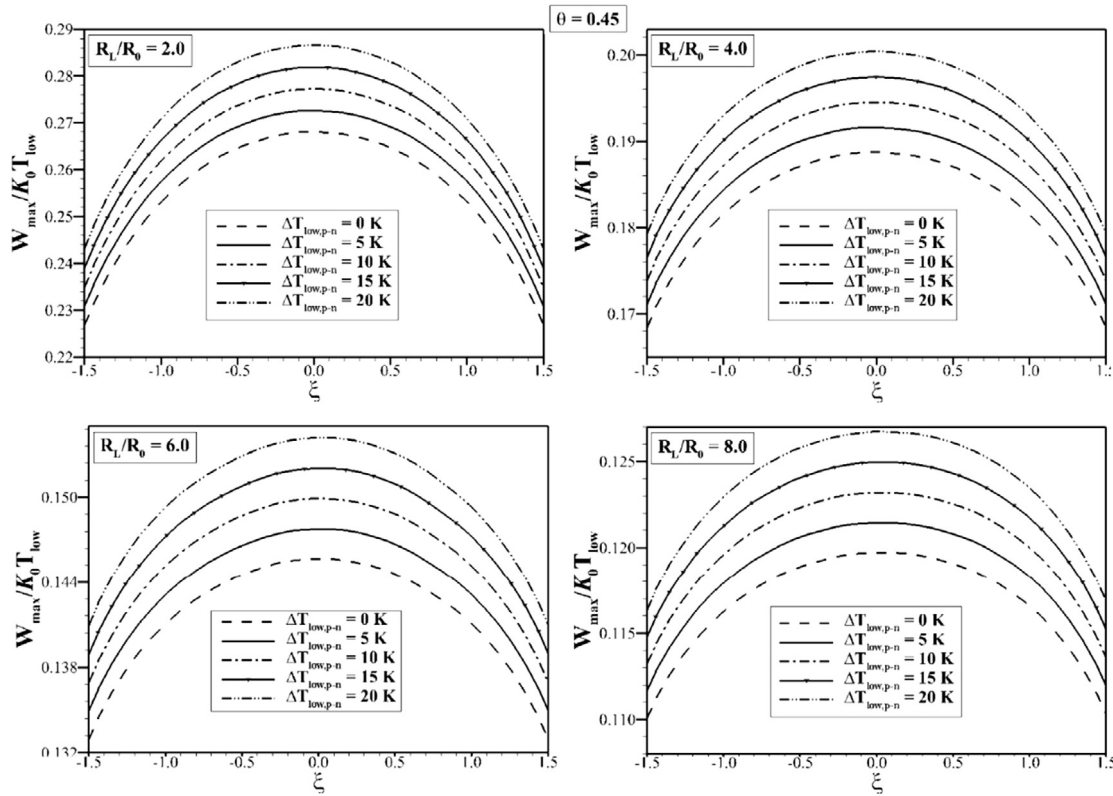


**Fig. 11a.** Variation of the maximum device output work with tapering parameter (shape factor,  $\xi = Ls/A_0$ ) for values of various external load ratio and cold junction temperature differences for temperature ratio  $\theta = 0.45$ .

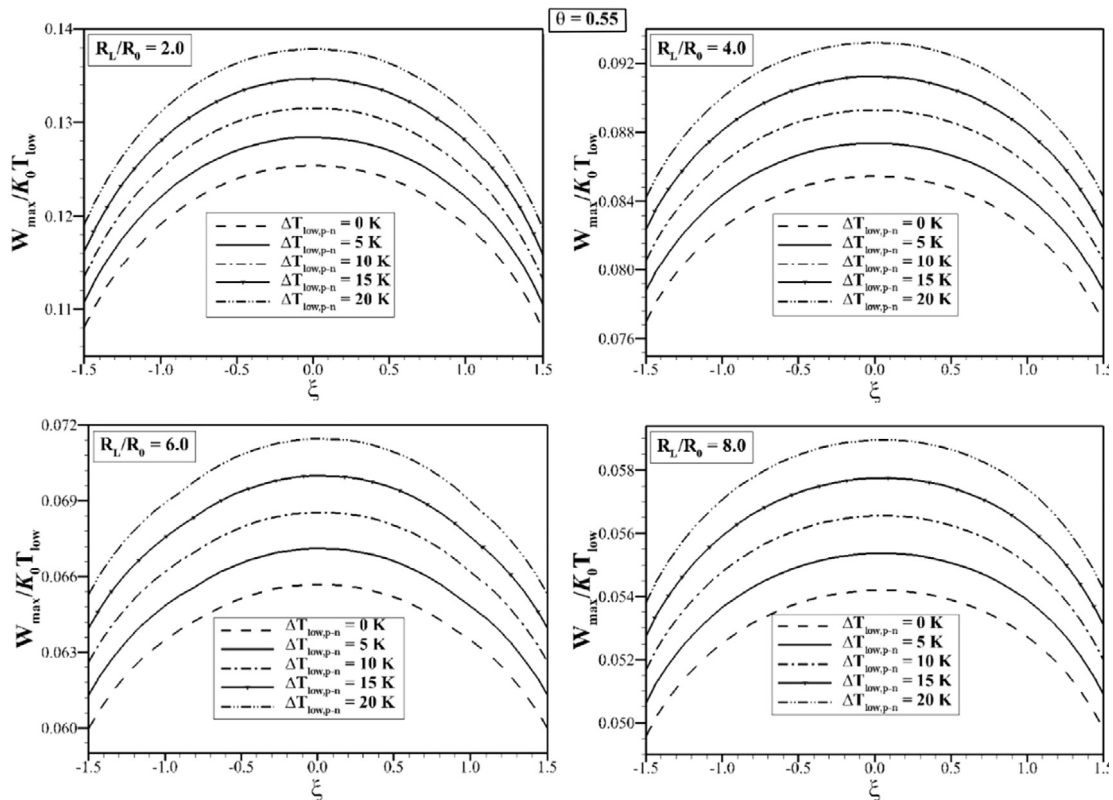


**Fig. 11b.** Variation of the maximum device output work with tapering parameter (shape factor,  $\xi = Ls/A_0$ ) for values of various external load ratio and cold junction temperature differences for temperature ratio  $\theta = 0.55$ .

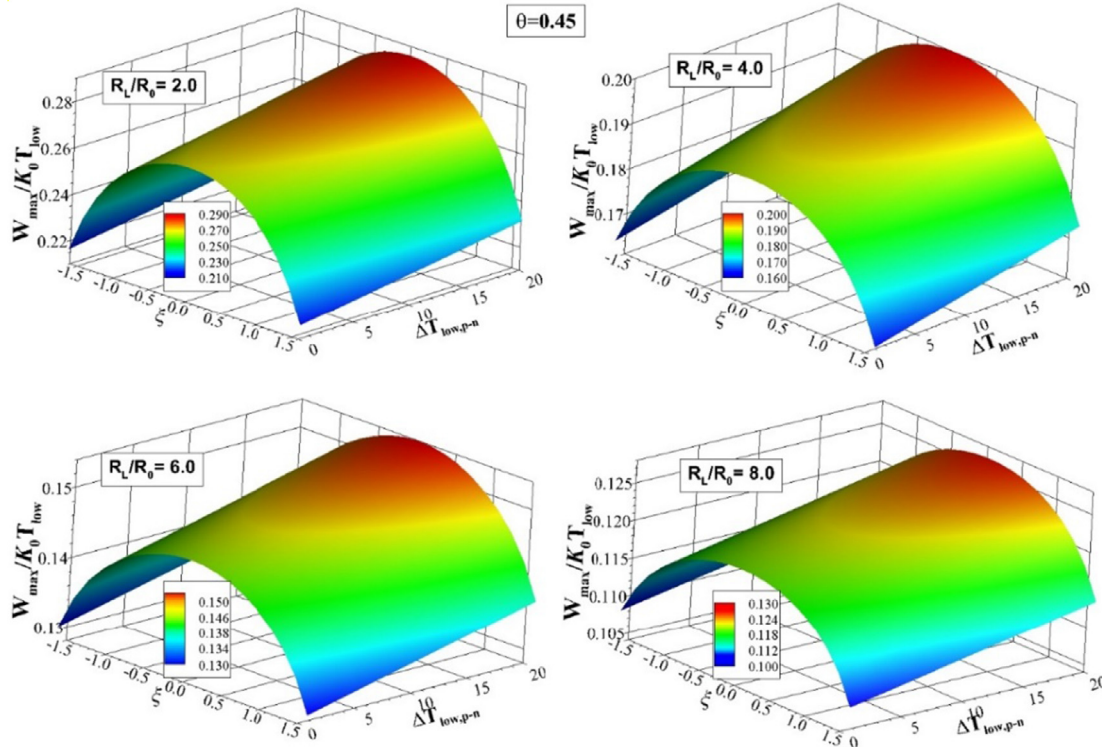


**Fig. 12a.** Surface plot of the maximum device output work with tapering parameter (shape factor,  $\xi = L_s/A_0$ ) and cold junction temperature differences for values of various external load ratio for temperature ratio  $\theta = 0.45$ .

moelectric generator provides higher output power than those classical design incorporating the single material. However, tapering of the pin configuration increases the output power ratio for all the cases considered, provided it reduces with tapering parameter

for small external load ratios ( $R_L/R_0 \leq 4$ ). The increase of the output power ratio indicates the reduction in the output power of the current design relative to those of the classical design with a single material pin configuration, particularly with increasing

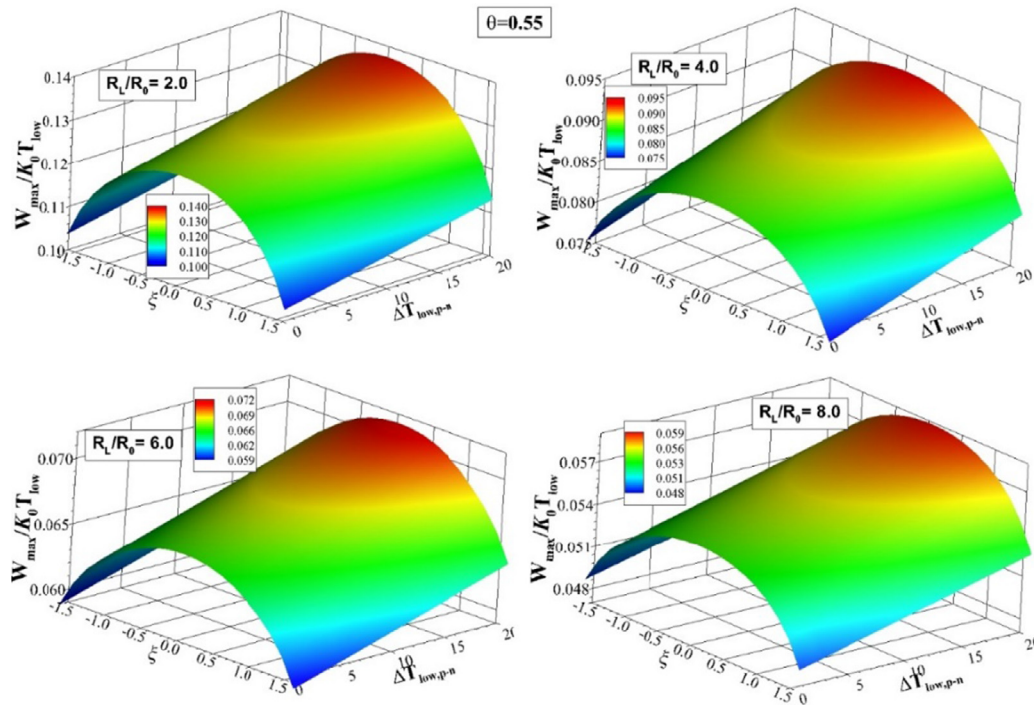


**Fig. 12b.** Surface plot of the maximum device output work with tapering parameter (shape factor,  $\xi = L_s/A_0$ ) and cold junction temperature differences for values of various external load ratio for temperature ratio  $\theta = 0.55$ .

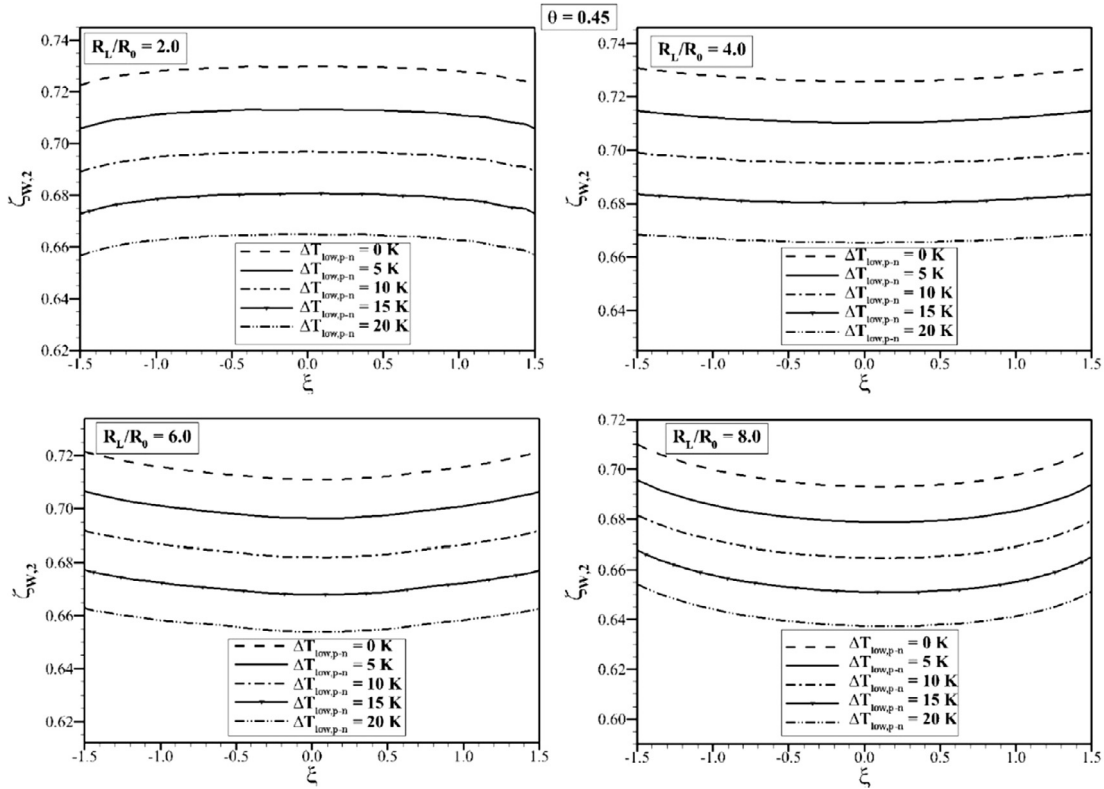


**Fig. 13a.** Variation of the output work ratio ( $\zeta_{W,2} = W_2 W_{\max}$ , where  $W_2$  is the output work of single material pin configuration – modified bismuth telluride) with tapering parameter for values of various external load ratio and cold junction temperature differences for temperature ratio  $\theta = 0.45$ .

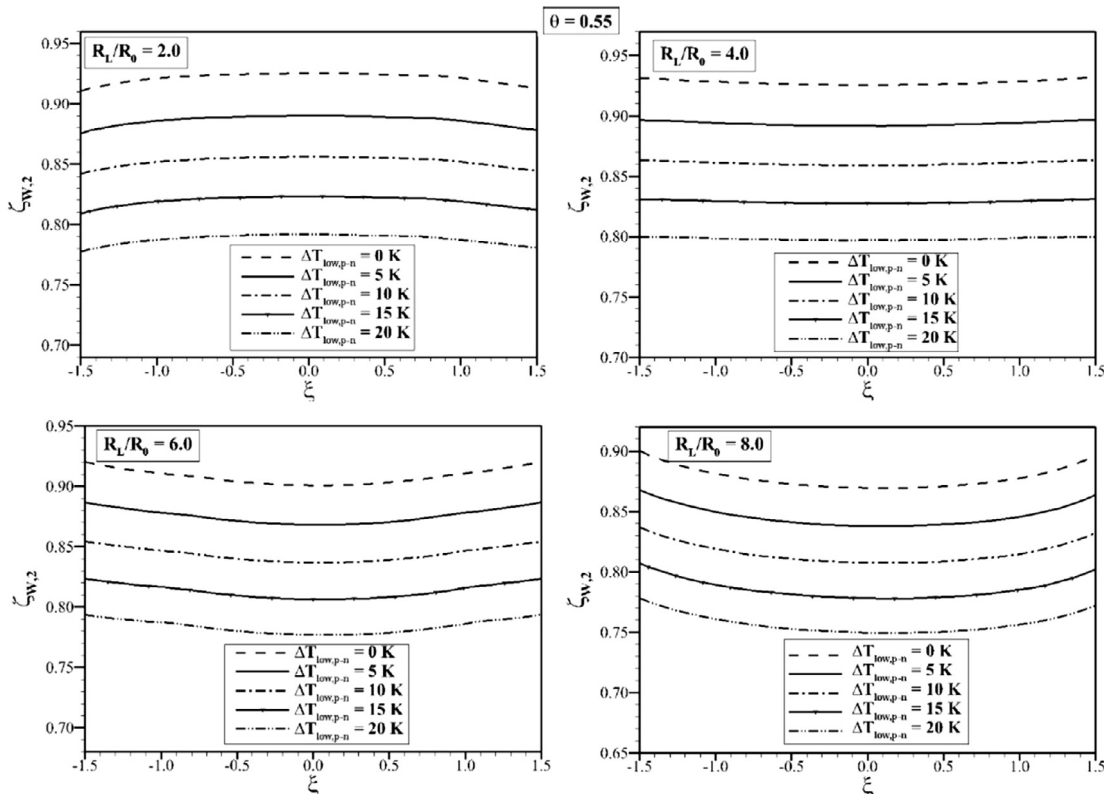


**Fig. 13b.** Variation of the output work ratio ( $\zeta_{W,2} = W_2 W_{\max}$ , where  $W_2$  is the output work of single material pin configuration – modified bismuth telluride) with tapering parameter for values of various external load ratio and cold junction temperature differences for temperature ratio  $\theta = 0.55$ .

tapering parameter. Nevertheless, this reduction is small. On the other hand, reducing external load ratio gives rise to increase of the output power ratio, which is particularly true with increasing tapering parameter. Consequently, depending on the external load ratio, tapering improves the output power of the new design as compared to those of the classical design with a single material pin configuration.

## 5. Conclusion

An innovative design of a thermoelectric generator is considered and thermodynamics analysis is carried out. The extended leg configuration with segmented and tapered pins is incorporated in the new design. Thermodynamic analysis is carried out and device efficiency and output power are presented in terms of device and operational parameters including the external load and temperature ratios. The performance of the thermoelectric device incorporating the new innovative design is compared to those of classical design using a single pin material configuration. It is found that the maximum efficiency of the device depends on the segmented and tapering configurations of the pin. In this case, increasing tapering improves the maximum efficiency. The operating parameters such as external load resistance and temperature ratios have a considerable effect on the maximum efficiency. This is particularly true for low value of the external load ratio ( $R_L/R_0 = 2$ ); in which case, the maximum efficiency increases notably. The new innovative design of extended leg configuration allows to operate the thermoelectric generator at two different cold junction temperatures. Increasing the cold junction temperature enhances the thermoelectric efficiency up to 8% increase. When comparing the efficiencies of the new innovative design of extended leg with segmented and tapered configuration with those of the classical designs incorporating the single material configurations, the new design of the thermoelectric generator results in improved thermal efficiency. This improvement signifies with the increased tapering of the pins. The device output power is influenced by the tapering, and the external load and temperature ratios. Increasing the tapering of the pins reduces the device output power slightly for the high values of the external load parameter ratio. However, the device output power increases with increasing tapering parameter of the pins for the case of external load parameter ratio  $R_L/R_0 \leq 4$ . Consequently, the device output power for the thermoelectric generator with tapered pin configuration depends on the operating conditions. When comparing the device output power corresponding to the new innovative design of the thermoelectric generator with those of the classical design incorporating the single material pin configuration, the new design of thermoelectric generator enhances the output power. This is true for all values of the tapering parameter and operating conditions of the thermoelectric generator.

## Acknowledgments

The authors acknowledge the funded project RG 1501 via support of Thermoelectric Group formed by the Deanship of Scientific Research at King Fahd University of Petroleum and Minerals, Dhahran, Saudi Arabia for this work.

## References

- [1] S. Li, J. Pei, D. Liu, L. Bao, J.-F. Li, H. Wu, L. Li, Fabrication and characterization of thermoelectric power generators with segmented legs synthesized by one-step spark plasma sintering, *Energy* 113 (2016) 35–43, <http://dx.doi.org/10.1016/j.energy.2016.07.034>.
- [2] H. Ali, B.S. Yilbas, F.A. Al-Sulaiman, Segmented thermoelectric generator: influence of pin shape configuration on the device performance, *Energy* 111 (2016) 439–452, <http://dx.doi.org/10.1016/j.energy.2016.06.003>.
- [3] G. Zhang, L. Fan, Z. Niu, K. Jiao, H. Diao, Q. Du, G. Shu, A comprehensive design method for segmented thermoelectric generator, *Energy Convers. Manage.* 106 (2015) 510–519, <http://dx.doi.org/10.1016/j.enconman.2015.09.068>.
- [4] H. Tian, N. Jiang, Q. Jia, X. Sun, G. Shu, X. Liang, Comparison of segmented and traditional thermoelectric generator for waste heat recovery of diesel engine, *Energy Procedia* (2015) 590–596, <http://dx.doi.org/10.1016/j.egypro.2015.07.461>.
- [5] H. Tian, X. Sun, Q. Jia, X. Liang, G. Shu, X. Wang, Comparison and parameter optimization of a segmented thermoelectric generator by using the high temperature exhaust of a diesel engine, *Energy* 84 (2015) 121–130, <http://dx.doi.org/10.1016/j.energy.2015.02.063>.
- [6] T. Ming, Y. Wu, C. Peng, Y. Tao, Thermal analysis on a segmented thermoelectric generator, *Energy* 80 (2015) 388–399, <http://dx.doi.org/10.1016/j.energy.2014.11.080>.
- [7] X. Jia, Y. Gao, Estimation of thermoelectric and mechanical performances of segmented thermoelectric generators under optimal operating conditions, *Appl. Therm. Eng.* 73 (2014) 333–340, <http://dx.doi.org/10.1016/j.aplthermaleng.2014.07.069>.
- [8] H.S. Kim, K. Kikuchi, T. Itoh, T. Iida, M. Taya, Design of segmented thermoelectric generator based on cost-effective and light-weight thermoelectric alloys, *Mater. Sci. Eng. B Solid-State Mater. Adv. Technol.* 185 (2014) 45–52, <http://dx.doi.org/10.1016/j.mseb.2014.02.005>.
- [9] C. Hadjistassou, E. Kyriakides, J. Georgiou, Designing high efficiency segmented thermoelectric generators, *Energy Convers. Manage.* 66 (2013) 165–172, <http://dx.doi.org/10.1016/j.enconman.2012.07.030>.
- [10] M.S. El-Genk, H.H. Saber, T. Caillat, Efficient segmented thermoelectric unicouples for space power applications, *Energy Convers. Manage.* 44 (2003) 1755–1772, [http://dx.doi.org/10.1016/S0196-8904\(02\)00217-0](http://dx.doi.org/10.1016/S0196-8904(02)00217-0).
- [11] L. Liu, X.S. Lu, M.L. Shi, Y.K. Ma, J.Y. Shi, Modeling of flat-plate solar thermoelectric generators for space applications, *Sol. Energy* 132 (2016) 386–394, <http://dx.doi.org/10.1016/j.solener.2016.03.028>.
- [12] B. Orr, A. Akbarzadeh, M. Mochizuki, R. Singh, A review of car waste heat recovery systems utilising thermoelectric generators and heat pipes, *Appl. Therm. Eng.* 101 (2016) 490–495, <http://dx.doi.org/10.1016/j.aplthermaleng.2015.10.081>.
- [13] B.S. Yilbas, H. Ali, Thermoelectric generator performance analysis: influence of pin tapering on the first and second law efficiencies, *Energy Convers. Manage.* 100 (2015) 138–146, <http://dx.doi.org/10.1016/j.enconman.2015.05.005>.
- [14] H. Ali, B.S. Yilbas, Configuration of segmented leg for the enhanced performance of segmented thermoelectric generator, *Int. J. Energy Res.* (2016), <http://dx.doi.org/10.1002/er.3620>.
- [15] B.W. Swanson, E.V. Somers, R.R. Heikes, Optimization of a sandwiched thermoelectric device, *J. Heat Transfer* 83 (1961) 77, <http://dx.doi.org/10.1115/1.3680473>.
- [16] J. D'Angelo, E.D. Case, N. Matchanov, C.-I. Wu, T.P. Hogan, J. Barnard, C. Cauchy, T. Hendricks, M.G. Kanatzidis, Electrical, thermal, and mechanical characterization of novel segmented-leg thermoelectric modules, *J. Electron. Mater.* 40 (2011) 2051–2062, <http://dx.doi.org/10.1007/s11664-011-1717-7>.